A&A 494, 949–967 (2009)
DOI: 10.1051/0004-6361:200811053

Astronomy & Astrophysics

Extremely faint high proper motion objects from SDSS stripe 82

Optical classification spectroscopy of about 40 new objects⋆

R.-D. Scholz[1], J. Storm[1], G. R. Knapp[2], and H. Zinnecker[1]

[1] Astrophysikalisches Institut Potsdam, An der Sternwarte 16, 14482 Potsdam, Germany
e-mail: [rdscholz;jstorm;hzinnecker]@aip.de
[2] Department of Astrophysical Sciences, Princeton University, Peyton Hall, Princeton, NJ 08544, USA
e-mail: gk@astro.princeton.edu

Received 29 September 2008 / Accepted 2 December 2008

ABSTRACT

Aims. By pushing the magnitude limit of high proper motion surveys beyond the limit of photographic Schmidt plates, we aim to discover nearby and very fast low-luminosity objects of different classes: cool white dwarfs (CWDs), cool subdwarfs (sd), and very low-mass stars and brown dwarfs at the very faint end of the main sequence (MS).
Methods. The deep multi-epoch Sloan Digital Sky Survey data in a 275 square degree area along the celestial equator (SDSS stripe 82) allow us to search for extremely faint ($i > 21$) objects with proper motions greater than 0.14 arcsec/yr. A reduced proper motion diagram $H_z/(i-z)$ clearly reveals three sequences (MS, sd, CWD) where our faintest candidates are representative of the still poorly known bottom of each sequence. We classify 38 newly detected objects with low-resolution optical spectroscopy using FORS1 @ ESO VLT. Together with our targets we observe six known L dwarfs in stripe 82, four (ultra)cool sd and one CWD as comparison objects. Distances and tangential velocities are estimated using known spectral type/absolute magnitude relations.
Results. All 22 previously known L dwarfs (and a few of the T dwarfs) in stripe 82 have been detected in our high proper motion survey. However, 11 of the known L dwarfs have smaller proper motions ($0.01 < \mu < 0.14$ arcsec/yr). Although stripe 82 was already one of the best investigated sky regions with respect to L and T dwarfs, we are able to classify 13 new L dwarfs. Two previously known L dwarfs have been reclassified by us. We have also found eight new M 7.5–M 9.5 dwarfs. The four new CWDs discovered by us are about 1–2 mag fainter than those previously detected in SDSS data. All new L-type, late-M and CWD objects show thick disk and halo kinematics. Since our high-velocity late-M and L dwarfs do not show indications of low metallicity in their spectra, we conclude that there may be a population of ultracool halo objects with normal metallicities. There are 13 objects, mostly with uncertain proper motions, which we initially classified as mid-M dwarfs. Among them we have found 9 with an alternative subdwarf classification (sdM7 or earlier types), whereas we have not found any new spectra resembling the known ultracool (>sdM7) subdwarfs. Some M subdwarf candidates have been classified based on spectral indices with large uncertainties.
Conclusions. We failed to detect new nearby ($d < 50$ pc) L dwarfs, probably because the SDSS stripe 82 area was already well-investigated before. With our survey we have demonstrated a higher efficiency in finding Galactic halo CWDs than previous searches. The space density of halo CWDs is according to our results about $1.5–3.0 \times 10^{-5}$ pc^{-3}.

Key words. stars: kinematics – stars: low-mass, brown dwarfs – stars: subdwarfs – strars: white dwarfs – Galaxy: halo – Galaxy: solar neighbourhood

1. Introduction

Deep sky surveys are not only important for the study of the most distant galaxies in the Universe but also for near-field stellar statistics and physics. It has been realised for a long time that the immediate Solar neighbourhood is the only region of a galaxy where there is a real chance for a complete survey of its stellar and sub-stellar content reaching to the lowest-luminosity objects. A complete volume-limited sample provides the groundwork for the knowledge of the local luminosity function, the mass function of field stars and brown dwarfs, and the Galactic star formation history (Reid et al. 2002; Gizis et al. 2002; Cruz et al. 2003). Moreover, the nearest representatives of a given class of objects can be considered as benchmark sources allowing detailed follow-up studies, including the search for possible planetary companions.

However, our knowledge of the Solar neighbourhood is still remarkably incomplete: Within a 25 pc horizon more than 60% of the stars (Henry et al. 2002) and probably more than 90% of the brown dwarfs remain to be discovered. The Research Consortium on Nearby Stars (RECONS) has documented the recent progress achieved for the 10 pc sample[1].

It should be noted that this sample is also not complete since it neglects recently discovered sources likely within 10 pc but without accurately measured parallaxes. It is defined as all known objects with trigonometric parallaxes of 100 mas or more, and an error in that parallax of less than 10 mas. An increase of about 20% has been achieved since 2000, so that the census has reached about 350 objects. About 240 of them are M dwarfs, which also contributed to the increase with the largest number (+40). The only other object classes with improved statistics are the L/T dwarfs and the planetary companions

⋆ Based on observations with VLT/FORS1 at the European Southern Observatory (ESO program 078.D-0595).

[1] http://www.chara.gsu.edu/RECONS/census.posted.htm

around nearby stars. The number of white dwarfs (18) has not changed, but there are ongoing efforts to find missing nearby white dwarfs (Subasavage et al. 2004, 2008). Subdwarfs represent the smallest group with only 4 objects in the 10 pc sample (Henry et al. 2006), all of which have been known for a long time, and which have extremely high proper motions ($3.7 < \mu < 8.7$ arcsec/yr).

Before time-consuming trigonometric parallax measurements can be started, one needs to know good nearby candidates of low-luminosity stars and substellar objects. Most nearby stars were first detected in high proper motion (HPM) surveys (e.g. Luyten 1979a,b; Luyten & Hughes 1980). HPM objects represent a mixture of *very nearby* neighbours of the Sun in the local population of the Galactic thin disk, and *very fast* representatives of the Galactic thick disk and halo, just passing through the neighbourhood. Although halo stars are relatively rare when compared to the number of disk stars in a local volume-limited sample, they are over-represented in HPM samples. The main observational material used in Luyten's HPM surveys were photographic Schmidt plates. Due to their full sky coverage in different colours and over long time intervals these archival data continue to play an important role in the search for nearby candidates. In particular, the deeper and partly redder (*I*-band) second epoch Schmidt survey plates by far have not yet been fully exploited to their limiting magnitudes.

The SuperCOSMOS Sky Surveys (SSS) represent one of the best available photographic archives suitable for the identification of hitherto unknown faint HPM stars, since they provide multi-colour catalogue data with cross-matching between the different passbands and epochs as well as images from the individual digitised photographic plates taken with three different Schmidt telescopes (Hambly et al. 2001a,b,c). The comparison of optical SSS data with near-infrared Two Micron All Sky Survey (2MASS; Skrutskie et al. 2006) data led to the discovery of new faint HPM objects with $\mu > 1$ arcsec/yr including some of the nearest brown dwarfs (Scholz et al. 2003; Kendall et al. 2007; Folkes et al. 2007), cool subdwarfs (Scholz et al. 2004a,b), late-type M dwarfs (Pokorny et al. 2003; Hambly et al. 2004), and cool white dwarfs (Scholz et al. 2002; Hambly et al. 2004).

New near-infrared sky surveys like the 2MASS and the DEep Near-Infrared Survey (DENIS; Epchtein et al. 1997) and deep multi-colour optical surveys like the Sloan Digital Sky Survey (SDSS; York et al. 2000) uncovered large numbers of objects cooler than the latest-type M dwarfs. New spectral classes, L (2500 K > $T_{\rm eff}$ > 1500 K) and T (1500 K > $T_{\rm eff}$ > 700 K), describing these ultracool objects, had to be defined less than ten years ago (Martín et al. 1999; Kirkpatrick et al. 1999; Burgasser et al. 2002; Geballe et al. 2002). Since then almost 650 L and T dwarfs have been discovered, mostly in 2MASS (≈50%) and SDSS (≈30%) (see Gelino et al. 2008, and references therein). About 50% of the L dwarfs and all T dwarfs in the Solar neighbourhood are brown dwarfs, whereas among late-M dwarfs only a few are sub-stellar objects (see review by Kirkpatrick 2005). Note that one of the latter is LP 944-20 (Tinney 1998), the only isolated brown dwarf already catalogued by Luyten (1979b; Luyten & Hughes 1980) as an HPM object, long before the first free-floating brown dwarfs were discovered from a new HPM survey by Ruiz et al. (1997) and from DENIS (Delfosse et al. 1997).

Cool, low-mass subdwarfs are interesting as tracers of Galactic structure and chemical evolution. They are metal-poor and typically exhibit halo kinematics (hence they show up preferentially in HPM surveys). The current classification scheme of cool subdwarfs ends at sdM7 (Gizis 1997). However, more and more cooler subdwarfs have been discovered in recent years (e.g. Lépine et al. 2003; Burgasser et al. 2003; Scholz et al. 2004a,b; Burgasser & Kirkpatrick 2006). A systematic search in the SDSS spectroscopic database has uncovered 23 new subdwarfs with spectral sub-types of M 7 or later and more than doubled the number of known ultracool subdwarfs (Lépine & Scholz 2008). There is some evidence that these so-called ultracool subdwarfs are somewhat hotter compared to normal dwarfs of the same spectral sub-type. Burgasser et al. (2007) derived 3100 K > $T_{\rm eff}$ > 2400 K for subdwarfs with spectral sub-types between M 7.5 and L4 from comparison with model spectra. An extension of the classification scheme for the ultracool subdwarfs, including sub-stellar subdwarfs, is now developing, where the spectral features indicating subtle changes in their physical properties (metallicity, surface temperature/clouds, gravity) are still under debate (Kirkpatrick 2005; Gizis & Harvin 2006; Lépine et al. 2007; Burgasser et al. 2007).

A third class of cool objects, completely different in their evolutionary stage and physical parameters from low-mass stars/brown dwarfs and cool subdwarfs, but also hard to detect due to their faintness, are the cool white dwarfs (CWDs). CWDs have long been considered as important objects for a number of reasons, such as determining the age of the Galactic disk (Leggett et al. 1998) and as possible components of the Galactic dark matter halo (Ibata et al. 2000; Oppenheimer et al. 2001; Méndez 2002; Flynn et al. 2003; Salim et al. 2004; Reid 2005). Among the coolest known CWDs ($T_{\rm eff}$ < 4500 K) in the Solar neighbourhood there are many objects already catalogued in the LHS (Luyten 1979a) or discovered as HPM objects from photographic plates (Hambly et al. 1997; Harris et al. 1999; Ibata et al 2000; Scholz et al. 2000; Monet et al. 2000; Scholz et al. 2002; Lépine et al. 2005; Carollo et al. 2006; Rowell et al. 2008). Other CWDs have been found in the SDSS (Harris et al. 2001; Gates et al. 2004; Kilic et al. 2006; Vidrih et al. 2007; Harris et al. 2008). Hall et al. (2008) found a nearby halo CWD with a large proper motion detected by combining the photographic USNO-B1.0 catalogue (Monet et al. 2003) with the SDSS (Munn et al. 2004). The space density of CWDs in the Galactic halo, possibly responsible for observed microlensing events, is still under debate (see e.g. Torres et al. 2008). Reid et al. (2001) had shown that the halo CWDs detected by Oppenheimer et al. (2001) in a HPM survey based on photographic Schmidt plates are in fact members of the thick disk. We conclude that a deeper HPM survey could either detect cooler objects or uncover the CWDs with even higher velocities, i.e. the real halo members.

As we have shown above, extending HPM surveys to fainter magnitude limits has led to the discovery of many benchmark sources of new classes of cool objects. Several new large-area HPM surveys relying *only* on modern deep optical (SDSS) and/or near-infrared (2MASS and SIMP) data have been successfully started (Artigau et al. 2006; Looper et al. 2007; Vidrih et al. 2007; Bramich et al. 2008; Metchev et al. 2008). The UKIRT Infrared Deep Sky Survey (UKIDSS; Lawrence et al. 2007) will eventually provide its own second epoch data suitable for HPM searches for the coolest brown dwarfs. The large-area survey of UKIDSS overlaps with SDSS, hence these different epoch data enable already deep HPM searches.

In this paper we present the first results of one of the deepest optical HPM searches done so far over a relatively large sky area. It is based on multi-epoch SDSS data in an equatorial stripe (called stripe 82) of about 275 square degrees. In Sect. 2 we describe our HPM survey and the selection of targets for follow-up observations. Section 3 deals with the spectroscopic classification of our extremely faint HPM objects. In Sect. 4 we discuss

their distance estimates and the resulting kinematics. In Sect. 5 we draw some conclusions and give the outlook on further work needed.

2. HPM survey and target selection

2.1. SDSS stripe 82

The SDSS consists of an imaging and spectroscopic survey over more than 25% of the sky (York et al. 2000). SDSS imaging data are taken simultaneously in the u, g, r, i, z bands (Fukugita et al. 1996; Gunn et al. 1998; Smith et al. 2002; Gunn et al. 2006) in drift-scan mode with a chip arrangement leading to a filled stripe of about 2.5 degrees width after two slightly overlapping scans (north and south strips). The data are pipeline-reduced, providing accurate astrometry (Pier et al. 2003) and photometry (Lupton et al. 1999, 2001; Hogg et al. 2001; Stoughton et al. 2002; Ivezic et al. 2004; Tucker et al. 2006; Padmanabhan et al. 2008). SDSS stripe 82 (hereafter S82) is the equatorial stripe (δ from -1.25 to $+1.25$ degrees) spanning 8 h in right ascension (α from $20^{\rm h}$ to $4^{\rm h}$). S82 north and south strips have been observed repeatedly, beginning in 1998. Since an imaging run may have covered all or part of a strip, about 250 square degrees in S82 were already covered by more than 20 SDSS imaging epochs until the end of 2004. This was the status in the SDSS database available at Princeton (Finkbeiner et al. 2004), which we considered as an excellent starting point for our search for faint moving objects.

Note that in our study we have not made use of the light and motion catalogues in S82 published by Bramich et al. (2008). Compared to the CWD candidates extracted from the latter by Vidrih et al. (2007), our HPM targets selected for VLT spectroscopy (see Sect. 2.2) are generally fainter by about one magnitude. Our S82 HPM survey was initiated in November 2005, about one year before a similar project by Bramich, Vidrih and coworkers was started. From the beginning of our independent S82 survey we were more interested in exploring the faintest possible HPM detections rather than in studying the whole HPM sample or presenting a complete catalogue. S82 data taken after the end of 2004, in particular the SDSS-II Supernova Survey (Frieman et al. 2008), were not included in our study.

We carried out our HPM survey primarily based on the SDSS multi-epoch imaging data in S82 taken between September 1998 and December 2004, but also using available 2MASS data for verification. This survey goes more than two magnitudes deeper compared to the SSS based southern sky HPM survey, which led to the discovery of the nearest brown dwarf, ε Indi B (Scholz et al. 2003), and also in comparison to the new complete northern sky HPM survey by Lépine & Shara (2005) based on photographic Schmidt plates. The high accuracy of SDSS single epoch astrometry has been demonstrated by Pier et al. (2003). These data allow us to determine proper motions, e.g. of faint brown dwarfs, if several epochs are available over a relatively short time interval of only few years (Finkbeiner et al. 2004).

Our HPM survey in S82 was carried out in stages:

1) we selected (due to restrictions in the computing power initially available for our task) a limited number of overlapping SDSS runs, well distributed in time (separated by about 6 months) over the full baseline of about six years. Tools described in Finkbeiner et al. (2004) were used to extract HPM candidates out of the Princeton SDSS database. A minimum of 5 epoch measurements was required to determine initial proper motions; typically 9 epochs over 3 to 6 years were used. The resulting survey area was about 275 square degrees;

2) all objects with initial proper motions above 0.2 arcsec/yr were then investigated in more detail in a second step involving all available SDSS epochs. For objects significantly brighter than the SDSS magnitude limits (a 95% detection repeatability for point sources is provided at $u = 22.0, g = 22.2, r = 22.2, i = 21.3, z = 20.5$) there were about 15 to 35 epochs, depending on the different overlap status within S82. However, objects at the SDSS magnitude limits, in which we were especially interested, did not appear on all available SDSS images. The proper motion fit was then checked visually, including a comparison of available 2MASS positions with the predicted position from the SDSS proper motion, to ensure that we select only real HPM objects. For the red objects ($i - z > 1$) we were able to extend the visual check to a lower proper motion limit of about 0.05 arcsec/yr. This was possible since the number of these candidates was not too large (less than a few thousand);

3) multi-epoch SDSS finding charts were inspected and data points with strongly deviating photometry were excluded from the proper motion fit in order to exclude doubtful HPM candidates. In particular, we excluded objects with matching problems between different epochs (close neighbors) and those of the faint objects, for which a large proper motion was caused by a *different position at only one epoch* (that may be two different objects at the SDSS magnitude limit).

2.2. Reduced proper motion diagram and i-magnitude cut

A reduced proper motion diagram (Fig. 1) is often used to separate the bottom of the main sequence (MS), the cool subdwarf (sd) sequence and the CWD sequence, when trigonometric distances and absolute magnitudes are not yet available (see e.g. Kilic et al. 2006; Carollo et al. 2006; Vidrih et al. 2007). The reduced proper motion (Hertzsprung 1905; Luyten 1922) is defined as $H = m + 5 + 5 \log \mu$, where m is the apparent magnitude and μ is the proper motion expressed in arcsec/yr. H can be used as a statistical equivalent of the absolute magnitude of a star in a sample with similar kinematics.

In Fig. 1 we have chosen an $H_z/(i - z)$ diagram to properly represent the L and T dwarfs, which are often barely detected in bluer SDSS passbands. The >1000 S82 HPM objects with $\mu > 0.14$ arcsec/yr found in step 1) of our survey (based on a limited number of epochs) with formal errors of less than 20 mas/yr are shown as dots. Some of these objects have spurious proper motions despite their formal small errors, as our later checking has shown. Three sequences (MS, sd, wd) are well separated. We aim to perform optical classification spectroscopy of the faintest new objects in all three sequences. For this reason, and in order to make good use of VLT observing time, we use an i-magnitude cut for our targets. The crosses represent the 38 faint targets (Table 1) finally selected after steps 2) and 3) of our HPM survey. These are all new HPM sources with $i > 21.5$, the majority of which have proper motions based on fewer than 15 individual epoch measurements, as well as some brighter objects ($21.0 < i < 21.5$) with typically more than 20 epochs. Table 1 lists accurate positions of our targets (finding charts can be obtained from the public SDSS DR6 webpage[2]), mean i and z magnitudes along with their errors, and the proper motion components with their errors together with the number

[2] http://cas.sdss.org/astrodr6/en/tools/chart/chart.asp

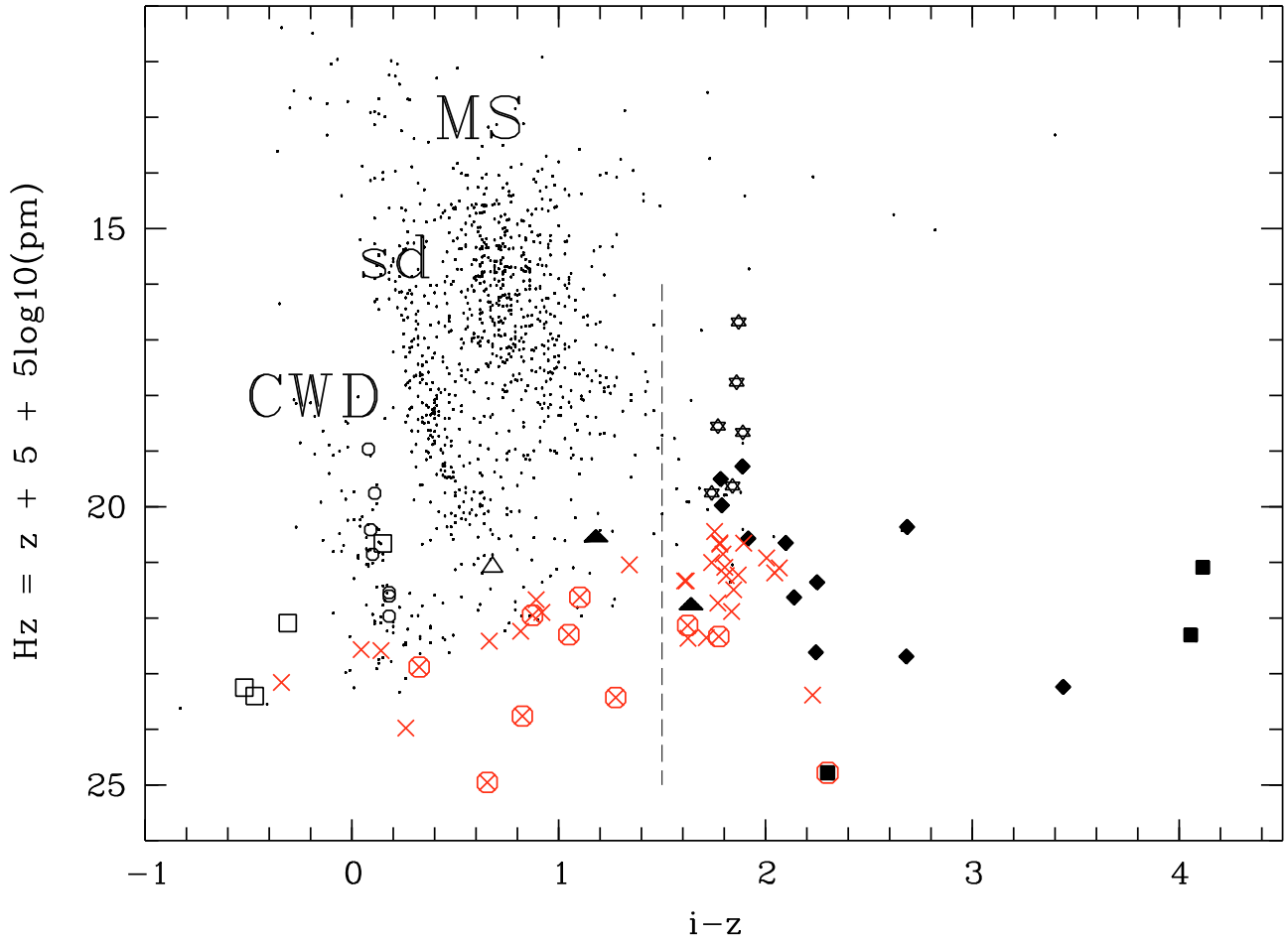

Fig. 1. Reduced proper motion diagram for objects with proper motions exceeding 0.14 arcsec/yr: all objects initially found after step 1) of our HPM survey (dots) with three separate sequences (MS, sd, CWD) marked, known L dwarfs (filled lozenges) and T dwarfs (filled squares) falling in the S82 survey area, M9 dwarfs (stars), L-type subdwarfs (filled triangles), a late-M extreme (esdM6.5) subdwarf (open triangle), CWDs (open circles and squares), and the confirmed faintest HPM objects after step 2) and 3) of our survey (crosses). Symbols overplotted by large open circles mark objects with uncertain proper motions (see Tables 1 and 2).

of epochs used for their determination. For one of our HPM discoveries (SDSS J013415.85+001456.0) the final proper motion solution (after excluding one outlier) led to a total value of about 0.13 arcsec/yr. All other new HPM objects have final proper motions higher than 0.14 arcsec/yr.

In the last column of Table 1 we have marked those objects that only have a few observations effectively distributed over only 2–4 different epochs or spread over a total time baseline of less than about four years. The very large proper motion errors of SDSS J231914.40+005615.9 are due to only five positions measured in two different seasons (two in autumn 2002 plus three in autumn 2003). However, both proper motion components are almost three times larger than the errors. This object has the largest value of the reduced proper motion shown in Fig. 1 ($H_z \approx 25$). All objects marked in the last column of Table 1 are overplotted with large open circles in Fig. 1. They occupy in particular the region of suspected subdwarfs. Although the marked objecs as well as some others with proper motion errors larger than ±25 mas/yr passed our 3-step procedure, we consider their large proper motions as relatively uncertain.

Other symbols shown in Fig. 1 represent the coolest known (in January 2006) objects of different classes from available SDSS data: L and T dwarfs from Gelino et al. (2008, and references therein), which all have $i - z$ colour indices larger than 1.5 (dotted line), M9 dwarfs from Hawley et al. (2002, their proper motions were determined by us), three cool subdwarfs from Lépine et al. (2003, 2004) and Sivarani et al. (2004; see also Burgasser et al. 2007), and two samples of CWDs discovered in SDSS, i.e. four CWDs with $\mu > 0.14$ arcsec/yr from Gates et al. (2004) and 7 CWDs with $T_{\rm eff} < 4000$ K and $\mu > 0.14$ arcsec/yr from Kilic et al. (2006).

One of the suspected L subdwarfs (the unpublished Sivarani object listed as sdL4: by Burgasser et al. 2007) falls in the region of the L/T dwarfs with $i-z > 1.5$, the other one (LSR 1610–0040, sdL:; Lépine et al. 2003), described by Cushing & Vacca (2006) as a very peculiar object (M6p/sdM), shows a much bluer colour typical of mid-M dwarfs. Very recently, a trigonometric parallax was measured for LSR 1610−0040 and it was found to be an astrometric binary of the Galactic halo population consisting of a mildly metal-poor M dwarf and a possible substellar companion (Dahn et al. 2008). The esdM6.5 object LSR J0822+1700 (Lépine et al. 2004) is much bluer and lies directly on the subdwarf sequence.

Half of our new targets are L dwarf candidates located in the region to the right of the dotted line ($i - z > 1.5$) in Fig. 1. From their position in the reduced proper motion diagram, there

Table 1. New faint HPM stars detected from SDSS S82 data.

Name from SDSS DR6 (SDSS J...)	α (J2000) [°]	δ (J2000) [°]	Epoch [year]	Mean i [mag]	Mean z [mag]	$\mu_\alpha \cos\delta$ [mas/yr]	μ_δ [mas/yr]	N_{ep}
(1)	(2)	(3)	(4)	(5)	(6)	(7)	(8)	(9)
002138.86+002605.8	005.411918	+00.434957	2002.6785	21.744 ± 0.045	19.934 ± 0.024	+161.4 ± 12.6	−84.6 ± 09.8	13
002800.37+010252.0	007.001579	+01.047793	2002.6785	21.637 ± 0.034	19.898 ± 0.022	+164.4 ± 10.6	−25.1 ± 15.6	32
003435.32+004633.9	008.647194	+00.776103	2001.7887	21.418 ± 0.042	19.664 ± 0.021	+136.9 ± 10.9	+42.2 ± 07.5	22
003550.48+004631.3	008.960348	+00.775378	2001.7887	21.923 ± 0.065	20.314 ± 0.042	+152.2 ± 14.4	−48.9 ± 13.8	23
005349.11−011354.4	013.454634	−01.231797	2002.6786	21.638 ± 0.052	19.860 ± 0.031	+144.7 ± 24.2	+15.0 ± 12.0	14
005636.22−011131.9	014.150936	−01.192200	2002.6786	22.118 ± 0.082	20.074 ± 0.062	−1.0 ± 16.6	−167.0 ± 31.1	13
005837.48+004435.6	014.656173	+00.743229	2001.7888	21.356 ± 0.046	19.731 ± 0.026	+311.6 ± 08.6	−126.0 ± 12.0	23
010959.91−010156.3	017.499632	−01.032308	2001.8897	21.985 ± 0.066	21.724 ± 0.118	+215.4 ± 23.9	−182.3 ± 20.3	22
011014.30+010619.1	017.559587	+01.105316	2001.8897	21.920 ± 0.044	19.692 ± 0.024	+546.2 ± 12.8	+41.4 ± 15.5	24
011755.09+005220.0⋆	019.479545	+00.872235	2003.8809	22.543 ± 0.121	20.919 ± 0.105	(+173.4 ± 33.6)	(+21.9 ± 30.6)	8†
013415.85+001456.0	023.566075	+00.248906	2001.8897	21.794 ± 0.026	20.453 ± 0.048	+77.9 ± 17.5	−105.6 ± 20.6	28
014956.27+001647.8	027.484491	+00.279958	2001.8898	21.412 ± 0.031	19.617 ± 0.019	+176.2 ± 09.0	+9.4 ± 07.2	30
020508.04+002458.7	031.283514	+00.416331	2002.6787	21.257 ± 0.023	21.212 ± 0.072	+184.5 ± 10.1	−28.2 ± 05.8	44
021546.76+010019.2	033.944852	+01.005350	2002.6787	21.906 ± 0.029	21.242 ± 0.108	−145.0 ± 27.3	−91.9 ± 27.6	15
024958.88+010624.3	042.495349	+01.106755	2001.8899	21.728 ± 0.036	20.837 ± 0.079	+106.5 ± 16.8	−101.0 ± 09.7	29
025316.06+005157.1	043.316948	+00.865881	2002.6788	22.036 ± 0.050	21.220 ± 0.088	+158.0 ± 37.6	−24.1 ± 19.6	11
032129.20+003212.8	050.371703	+00.536911	2002.6789	21.446 ± 0.025	21.305 ± 0.093	+120.2 ± 10.0	−134.4 ± 08.0	21
033203.57+003658.0⋆	053.014867	+00.616101	2003.7330	22.272 ± 0.054	21.223 ± 0.130	(+164.1 ± 26.3)	(+1.3 ± 13.1)	8†
033456.32+010618.7	053.734696	+01.105197	2001.8900	21.048 ± 0.024	19.334 ± 0.015	+387.0 ± 07.5	−107.6 ± 06.0	32
204821.28−004734.1	312.088698	−00.792822	2001.7200	21.558 ± 0.057	20.734 ± 0.166	(−255.8 ± 28.6)	(+311.8 ± 30.3)	7†
213151.87−001432.4	322.966158	−00.242351	2001.7201	21.521 ± 0.027	19.742 ± 0.032	+17.0 ± 21.3	−150.9 ± 24.3	12
215322.18−004553.9	328.342427	−00.764994	2002.7768	22.453 ± 0.228	21.178 ± 0.140	(+43.1 ± 32.6)	(−278.6 ± 56.8)	6†
215351.20+010120.3	328.463332	+01.022322	2002.7768	21.884 ± 0.042	20.965 ± 0.149	(+53.0 ± 15.5)	(−144.3 ± 35.2)	10†
215515.49+005128.0	328.814572	+00.857790	2002.7768	21.879 ± 0.060	20.777 ± 0.076	(+133.4 ± 22.3)	(−63.5 ± 22.0)	11†
215817.69+000300.3	329.573715	+00.050106	2002.7768	21.717 ± 0.055	19.822 ± 0.039	+88.5 ± 16.6	−117.0 ± 18.9	13
215934.25+005308.5	329.892736	+00.885709	2002.7768	22.232 ± 0.101	20.396 ± 0.052	+191.8 ± 28.9	−50.4 ± 20.6	11
220952.49+003325.2⋆	332.468692	+00.557009	2004.8391	21.928 ± 0.055	21.055 ± 0.199	(+94.3 ± 33.9)	(−118.0 ± 25.6)	6†
221911.35+010220.5	334.797303	+01.039031	2002.7769	21.667 ± 0.032	21.341 ± 0.140	(+200.6 ± 38.6)	(−32.1 ± 81.7)	9†
222939.14+010405.5	337.413111	+01.068200	2001.7885	21.547 ± 0.054	21.888 ± 0.170	+177.5 ± 11.8	−25.7 ± 14.7	15
225903.29−004154.2	344.763708	−00.698389	2002.7769	22.080 ± 0.069	20.305 ± 0.062	(−51.8 ± 44.0)	(−249.0 ± 29.9)	8†
230722.58−005746.6	346.844120	−00.962948	2001.7886	22.189 ± 0.052	20.183 ± 0.031	+129.1 ± 21.7	−55.3 ± 13.9	23
231407.82+004908.2	348.532598	+00.818961	2001.7886	21.736 ± 0.055	20.120 ± 0.029	+103.8 ± 14.8	−140.7 ± 13.2	25
231914.40+005615.9	349.810022	+00.937755	2002.6784	22.061 ± 0.095	21.406 ± 0.241	(+289.2 ± 98.9)	(−422.8 ± 152.)	5†
232935.99−011215.3	352.399971	−01.204256	2002.6784	22.073 ± 0.074	20.270 ± 0.034	+143.0 ± 25.8	−27.7 ± 19.1	14
234841.38−004022.1	357.172419	−00.672832	2002.6784	21.999 ± 0.051	19.932 ± 0.052	+108.9 ± 16.0	−132.1 ± 18.7	15
235826.48+003226.9	359.610344	+00.540813	2002.6785	22.218 ± 0.068	20.448 ± 0.044	+179.9 ± 31.7	−14.7 ± 21.3	11
235835.45−000909.5	359.647731	−00.152658	2001.7887	21.120 ± 0.020	19.252 ± 0.014	−96.5 ± 10.2	−228.7 ± 09.6	20
235841.98+000622.0	359.674927	+00.106135	2002.6785	21.975 ± 0.049	20.129 ± 0.046	+168.9 ± 27.5	−80.9 ± 20.3	11

Notes: Names, coordinates and epochs are taken from SDSS data release 6 (DR6; Adelman-McCarthy et al. 2008) except for three objects marked by ⋆, for which due to the lack of DR6 data the latest available (in our analysis) epoch position from S82 is given instead. Objects marked by † in Col. (9) had observations spread over only 2–4 different epochs or less than about 4 years, thus their proper motions (in parentheses) are uncertain.

could also be a T dwarf among these candidates, since the known three objects exhibit a large spread in the $i - z$ colour indices. Although M 8 and M 9 dwarfs also have average $i - z$ colour indices between 1.6 and 1.7 (West et al. 2005), we do not expect a high contamination of our sample by late-M dwarfs, since the M9 dwarfs with similarly large proper motions lie clearly above all our selected faint VLT targets in the reduced proper motion diagram. Our candidates with $0.5 < i - z < 1.5$ show a wide-spread apparent extension of the subdwarf sequence. On the blue side ($i - z < 0.5$) there are some good candidates for new benchmark sources among the coolest white dwarfs.

2.3. Comparison objects

In Table 2 we list all L and T dwarfs discovered until now in the S82 region from different surveys, not just the SDSS. The first column gives the discovery name marked with the corresponding reference (comparison objects selected by us as additional targets for our spectroscopic observations are marked by #), the following columns list J magnitudes (2), optical spectral types with references (3), near-infrared spectral types with references (4) (all data taken from Gelino et al. 2008, where the J magnitudes of all objects brighter than 17.5 are from 2MASS, whereas fainter J magnitudes are from the discovery papers). In the last five columns we give the mean i and z magnitudes (5, 6) and the proper motion components (7, 8) derived by us using the number of SDSS epochs listed in the last Col. (9).

At the beginning of our HPM survey (November 2005), there were 24 known L/T dwarfs falling in the S82 area. Out of these we were able to re-discover all but two as HPM objects (Table 2). One of the latter (SDSSp J030321.24−000938.2) was classified by Schneider et al. (2002) as an L0 dwarf, which however

Table 2. Known L and T dwarfs in S82 and their new SDSS-based mean i and z magnitudes and proper motions.

Discovery name ($^{\#}$ = comparison objects) (1)	J [mag] (2)	Opt. SpT (3)	IR SpT (4)	Mean i [mag] (5)	Mean z [mag] (6)	$\mu_\alpha \cos\delta$ [mas/yr] (7)	μ_δ [mas/yr] (8)	N_{ep} (9)
SDSS J001608.44−004302.3[1]	16.326 ± 0.116		L5.5[1]	21.276 ± 0.024	19.213 ± 0.029	+129.2 ± 08.8	−16.7 ± 10.2	11
SDSS J001911.65+003017.8[2]	14.921 ± 0.037	L1[2]		19.353 ± 0.014	17.534 ± 0.006	−17.7 ± 08.9	−59.1 ± 11.8	12
ULAS J002422.94+002247.9[3]	18.160 ± 0.070		T4.5[3]					
ULAS J003402.77−005206.7[4]	18.140 ± 0.080		T8.5[4]					
2MASS J00521232+0012172[5,#]	16.361 ± 0.108		L2p ± 1[5]	21.651 ± 0.025	19.401 ± 0.016	-161.0 ± 10.0	−186.2 ± 07.9	32
SDSSp J005406.55−003101.8[6,#]	15.731 ± 0.053	L1[2]		20.131 ± 0.011	18.214 ± 0.006	+235.5 ± 11.2	−179.5 ± 06.6	21
CFBDS J005910.90−011401.3[7]	18.060 ± 0.030		T9[7]					
2MASSI J0104075−005328[8,#]	16.531 ± 0.130	L4.5[15]		21.578 ± 0.038	19.334 ± 0.024	+453.1 ± 08.9	-10.1 ± 10.1	15
SDSSp J010752.33+004156.1[9,#]	15.824 ± 0.058	L8[2]	L5.5[1]	21.331 ± 0.028	18.650 ± 0.010	+637.5 ± 06.0	+81.0 ± 05.7	24
ULAS J013117.53−003128.6[10]	18.600 ± 0.040		T3[10]					
ULAS J013939.77+004813.8[10]	18.430 ± 0.040		T7.5[10]					
SDSS J020333.26−010812.5[1]	16.858		L9.5[1]	23.889 ± 0.324	20.450 ± 0.043	+361.0 ± 18.3	+5.2 ± 18.8	13
ULAS J020336.94−010231.1[3]	18.040 ± 0.050		T5[3]					
SDSS J020742.48+000056.2[9]	16.799 ± 0.156		T4.5[13]	24.372 ± 0.266	20.258 ± 0.038	+143.8 ± 15.8	−28.2 ± 10.5	20
IfA 0230−Z1[11]	18.200		T3[13]	23.414:	21.104:	(+430:)	(+325:)	1[†]
SDSS J022723.77−005518.6[2]	16.877	L0[2]		21.013 ± 0.017	19.341 ± 0.012	+46.4 ± 06.8	−9.5 ± 07.1	32
SDSSp J023617.93+004855.0[9,#]	16.098 ± 0.077	L6[2]	L6.5[1]	21.501 ± 0.029	18.816 ± 0.008	+133.9 ± 05.7	−153.7 ± 06.5	32
SDSS J025601.86+011047.2[2]	16.212 ± 0.102	L0[2]		20.502 ± 0.011	18.719 ± 0.009	+125.7 ± 13.0	−69.0 ± 14.7	33
SDSSp J030136.53+002057.9[6]	16.882 ± 0.190	L1:[6]		21.012 ± 0.014	19.199 ± 0.014	+73.4 ± 06.3	−77.9 ± 07.2	31
SDSSp J030321.24−000938.2[6]	16.120 ± 0.072	L0[6,*]		20.184 ± 0.010	18.308 ± 0.006	+12.4 ± 11.2	+9.7 ± 08.6	32
SDSSp J032817.38+003257.2[6]	15.988 ± 0.092	L3[2]		20.587 ± 0.010	18.798 ± 0.011	+171.1 ± 06.5	+17.5 ± 07.4	22
SDSSp J033017.77+000047.8[6]	16.520 ± 0.111	L0:[6]		20.637 ± 0.017	18.861 ± 0.010	−38.2 ± 13.6	−75.4 ± 15.4	21
SDSSp J033035.13−002534.5[12]	15.311 ± 0.050	L4[2]		20.155 ± 0.007	18.017 ± 0.008	+392.4 ± 10.8	−352.4 ± 07.2	25
ULAS J034832.97−001258.3[10]	18.720 ± 0.040	early T[10]						
SDSS J035448.73−002742.1[1]	17.282 ± 0.211		L2 ± 1[1]	21.513 ± 0.017	19.554 ± 0.016	+45.9 ± 08.0	−42.9 ± 05.1	27
SDSS J202820.32+005226.5[2]	14.298 ± 0.035	L3[2]		18.787 ± 0.022	16.997 ± 0.001	+135.3 ± 18.0	+14.7 ± 08.1	4
SDSS J212413.89+010000.3[1]	16.031 ± 0.074		T5[13]	23.701 ± 0.573	19.645 ± 0.046	+237.6 ± 31.6	+243.5 ± 17.5	12
SDSS J214046.55+011259.7[2,#]	15.891 ± 0.084	L3[2]		21.063 ± 0.032	18.965 ± 0.017	−71.6 ± 11.1	−205.1 ± 05.2	15
ULAS J222958.30+010217.2[10]	17.880 ± 0.020		T2.5[10]					
ULAS J223955.76+003252.6[3]	18.850 ± 0.050		T5.5[3]					
SDSSp J224953.45+004404.2[9]	16.587 ± 0.125	L3[2]	L5 ± 1.5[1]	21.635 ± 0.045	19.477 ± 0.021	+88.8 ± 09.8	+17.8 ± 09.2	16
SDSSp J225529.09−003433.4[6]	15.650 ± 0.056	L0:[6]		19.814 ± 0.008	17.925 ± 0.007	−48.7 ± 14.5	−179.9 ± 15.6	17
SDSS J225913.88−005158.2[2]	16.357 ± 0.098	L2[2]		20.757 ± 0.016	18.985 ± 0.013	+46.1 ± 09.8	+29.2 ± 12.7	22
2MASS J23453903+0055137[14]	13.771 ± 0.030	L0[16]		18.001 ± 0.003	16.171 ± 0.005	+93.4 ± 06.8	−67.1 ± 11.6	16

References: [1] Knapp et al. (2004); [2] Hawley et al. (2002); [3] Lodieu et al. (2007); [4] Warren et al. (2007); [5] Metchev et al. (2008); [6] Schneider et al. (2002); [7] Delorme et al. (2008); [8] Berriman et al. (2003); [9] Geballe et al. (2002); [10] Chiu et al. (2008); [11] Liu et al. (2002); [12] Fan et al. (2000); [13] Burgasser et al. (2006); [14] Reid et al. (in prep); [15] Kirkpatrick et al. (in prep); [16] unpublished; [*] may be a distant red giant according to our non-significant proper motion; [†] uncertain proper motion (see text).

according to our measurements has a zero proper motion (we speculate this may be a distant red giant). For the other, a faint T dwarf (IfA 0230−Z1), there was only only one epoch measurement available in S82 (with $i = 23.414, z = 21.104$). The comparison of the SDSS position of IfA 0230−Z1 with the position given in the discovery paper by Liu et al. (2002) hints at a high proper motion of $(\mu_\alpha \cos\delta, \mu_\delta) \approx (+430, +325)$ mas/yr. If its spectral classification and our SDSS identification are correct, then this is a T dwarf with a large reduced proper motion ($H_z = 24.8$) and a relatively blue colour ($i - z = +2.30$; see Fig. 1). According to our measurements many of the known early-L dwarfs have proper motions lower than 0.14 arcsec/yr and are therefore not shown in Fig. 1.

Note that the number of L and T dwarfs coincident with the S82 area, which was already one of the best investigated sky areas with respect to these object classes, has further increased since the beginning of our survey. The current number is 34 according to the status of 22 April 2008 in the DwarfArchives (Gelino et al. 2008). This corresponds to an eight times higher surface density of L and T dwarfs in S82 compared to the formal all-sky value simply computed from the 649 currently known objects (Gelino et al. 2008). One new L dwarf was discovered in S82 by Metchev et al. (2008). This object was independently found by us in our HPM survey and originally selected as a promising new target for our spectroscopic observations. We use it now as an additional known comparison object, although it has only a near-infrared spectral type. Eight T dwarfs were discovered by Warren et al. (2007), Lodieu et al. (2007), and Chiu et al. (2008) from UKIDSS data. One of the coolest known brown dwarfs, discovered from a deep imaging survey with the Canada-France-Hawaii Telescope (Delorme et al. 2008), is also located in S82. All the new T dwarfs are too faint ($J > 17.5$) so that we were not able to detect them in our SDSS-based HPM survey.

In addition to the 6 known L dwarfs included as comparison objects (Table 2), we selected four known cool subdwarfs as "standard stars" for our spectroscopic observations: SDSS J125637.12−022452.4 (sdL4:; Sivarani et al. 2004; Burgasser et al. 2007), LSR 1610−0040 (M6p/sdM; Lépine et al. 2003;

Cushing & Vacca (2006), SSSPM J1013−1356 (sdM9.5; Scholz et al. 2004a), and LEHPM 2–59 (esdM8; Pokorny et al. 2004; Burgasser & Kirkpatrick 2006). Finally, one of the coolest known white dwarfs was included in our spectroscopy target list: SDSSp J133739.40+000142.8 (Harris et al. 2001).

3. Optical classification spectroscopy

The existing spectroscopic classification schemes for L dwarfs, cool subdwarfs and CWDs work best in the optical wavelength region. Therefore, a first look in the optical seems to be justified in order to classify our new, extremely faint HPM discoveries. In the following we describe the spectroscopic observations, data reduction, and the classification of our targets based on spectral indices and comparison with spectra of known objects of different classes.

3.1. Observations and data reduction

Low-resolution spectroscopy was obtained over 25 h of service observations with the ESO VLT Keuyen telescope and the FORS1 instrument (Appenzeller et al. 1998) during period 78 (October 2006 to March 2007). We used grism GRIS_150I+17 with a wavelength range of 600–1100 nm, and a dispersion of 23 nm/mm. The slit, set to the parallactic angle, had a width of 1 arcsec, and the seeing varied between 0.45 and 1.4 arcsec with a few spectra with worse seeing. With 44 faint targets, including 38 new objects (Table 1) and 6 known L dwarfs (Table 2) the effective exposure times for the spectra ranged typically between 13 and 23 mn. For 5 brighter ($16 < i < 19.5$) comparison objects, including one CWD and four late-type subdwarfs, only relatively short exposure times of one to five minutes were needed.

The spectra were bias subtracted, flat-fielded and wavelength calibrated before they were extracted using the optimal extraction algorithm within the IRAF[3] `onedspec` package. The spectra were flux-calibrated using spectra of four standard stars (Feige 100, LTT 2415, LTT 1020, & LTT 3218) with spectrophotometry from Hamuy et al. (1994) and using the CTIO extinction curve provided within IRAF. As the spectra were obtained on many different nights we do not have appropriate nightly calibration spectra and due to the fairly low signal to noise ratio it was not reasonable to attempt to scale and subtract a standard telluric spectrum from the data.

The spectra of all targets and comparison objects are normalised at 7500 Å and are shown on the same scale in Fig. 2 (CWDs, M (sub)dwarfs and ultracool subdwarfs) and Fig. 3 (L dwarfs), respectively sorted by spectral types. The spectra of our comparison objects are marked by #.

3.2. L and M spectral types

For the spectral typing of our targets we first used the visual comparison of their spectra with those of the known comparison objects. A surprisingly large number of our targets looked like the peculiar (sub)dwarf LSR 1610−0040 (M6p/sdM) while their continuum was not that red. Since we had not included normal mid- to late-type M dwarfs in our observations, we selected in addition to our own template VLT/FORS1 spectra a sequence of M dwarf spectra (observed with Keck/LRIS) from the spectral library provided by Reid[4] for our comparison.

Although the signal-to-noise and resolution of our spectra are rather low, we also used the measurements of spectral indices in order to classify our objects. In particular, we measured the TiO5 index defined by Reid et al. (1995), the VOa index defined by Kirkpatrick et al. (1999), and the PC3 index defined by Martín et al. (1999). The spectral indices together with their errors determined from the standard deviations of flux values in the corresponding wavelength intervals are listed in Table 3. We then applied the spectral type versus spectral index relation for TiO5 and VOa given by Cruz & Reid (2002) and for PC3 given by Martín et al. (1999). The results are shown in Table 4, where the average spectral types based on spectral indices, the spectral types based on visual comparison, and the finally adopted spectral types are shown in Cols. 8–10, respectively. Note that there are also alternatively adopted subdwarf types given in Col. 10 for nine of the objects initially classified as M 3–M 6 (see Sect. 3.3).

The relatively large errors of the individual spectral indices and the corresponding spectral types, as well as the whole procedure for determining spectral types (as a weighted mean of index-based and visual results) were in general similar to the errors and the method used in Phan-Bao et al. (2008). However, there are some differences: 1) We used the formula for L 1–L 6 dwarfs from Martín et al. (1999) when the PC3 index was larger than 2.5, as was also done by Martín et al. (2006); 2) For the final spectral types, we took the average of two values, of the spectral type determined on the one hand from visual comparison with template spectra, and of the mean spectral type obtained on the other hand from the three (PC3, TiO5, VOa) spectral indices. The uncertainty of the finally adopted spectral types is conservatively estimated as one spectral type.

In the case of the new L 4 dwarf SDSS J011014.30+010619.1 we did not use the spectral type corresponding to the TiO5 index in the computation of the finally adopted spectral type. This object has not only one of the highest uncertainties in its TiO5 index, but the index is also much larger than the upper limit (1.5) shown in the spectral index/spectral type relation of Cruz & Reid (2002; their Fig. 3). For the two comparison late-L dwarfs, we have not used the average of index-based spectral types, as the Cruz & Reid (2002) spectral type/spectral index relations are only valid up to mid-L types. For all our comparison objects we adopted the previously known optical spectral types (Table 2), except for our latest-type object SDSSp J023617.93+004855.0, which we re-classified based on the comparison with the spectrum of the L 8 dwarf SDSSp J010752.33+004156.1 (Fig. 3) as an L 9 dwarf (see also Sect. 4). The spectrum of 2MASS J00521232+0012172, for which only a near-infrared spectral type was known before (Table 2), is very similar to that of the L 4.5 dwarf 2MASSI J0104075−005328 and was also classified as L4.5 based on its spectral indices.

We have compared the results from the visual spectral classification using normal M and L dwarf templates with those based on the spectral indices (Fig. 6) and found small systematic differences. For all 37 objects investigated, we found a mean difference (visual minus index-based) of +0.46 (with a standard deviation of 0.76) subtypes. A larger difference of +0.69 (st. dev. 0.44) is measured for 12 M 3–M 6 dwarfs, whereas the effect is smaller for the 25 M 7–L 5 dwarfs: +0.35 (st. dev. 0.85). The largest individual differences reach 1.6 and 1.9 subtypes, respectively, for the M 3–M 6 and M 7–L 5 dwarfs. We note that the

[3] IRAF is the Image Reduction and Analysis Facility, made available to the astronomical community by the National Optical Astronomy Observatories, which are operated by AURA, Inc., under cooperative agreement with the National Science Foundation.

[4] http://www.stsci.edu/~inr/ultracool.html

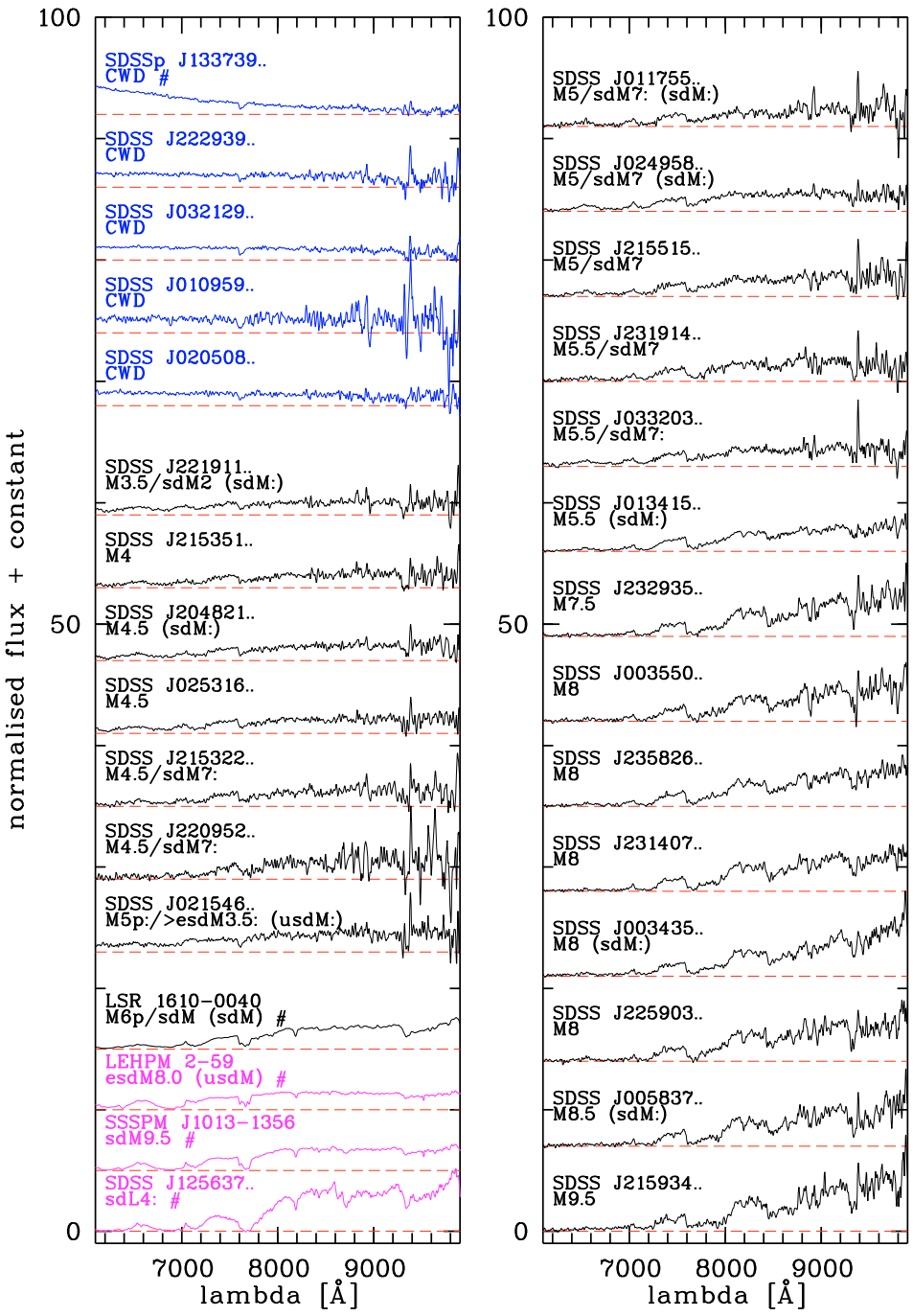

Fig. 2. VLT/FORS1 spectra of cool white dwarfs (five spectra in *upper part of left column*), comparison late-type (M/L) subdwarfs (four spectra in *lower part of left column*, including three ultracool >sdM7 subdwarfs), and M dwarfs/subdwarfs sorted by spectral type (*middle of left column and right column*). Subdwarf candidates indicated in brackets were determined according to the revised metallicity classes (sdM, esdM, usdM) defined by Lépine et al. (2007). Comparison objects with previously known spectral types are marked by #. All spectra are normalised at 7500 Å and smoothed with a running mean over 7 pixels.

PC3 index alone already gives very similar results to our visual classification. The two other indices show a much larger scatter and different systematic deviations, which however compensate for each other in the averaging. The small systematic errors and standard deviations given above are well below our conservatively estimated classification accuracy of one spectral type and show that the two methods (index-based and visual) lead to similar results.

In total, we classified 13 new L dwarfs and assigned new spectral types to two previously known L dwarfs from our optical spectra. We also found 8 new late-type M dwarfs and 13 mid-type M dwarfs. In the following we have searched for subdwarf candidates among the M-type objects.

3.3. M (sub)dwarfs

From the visual comparison of the new target spectra with the comparison cool subdwarf spectra shown in the lower left part of Fig. 2 we did not find any obvious similarities. In particular, none of the late-M and L-type spectra resembled one of the

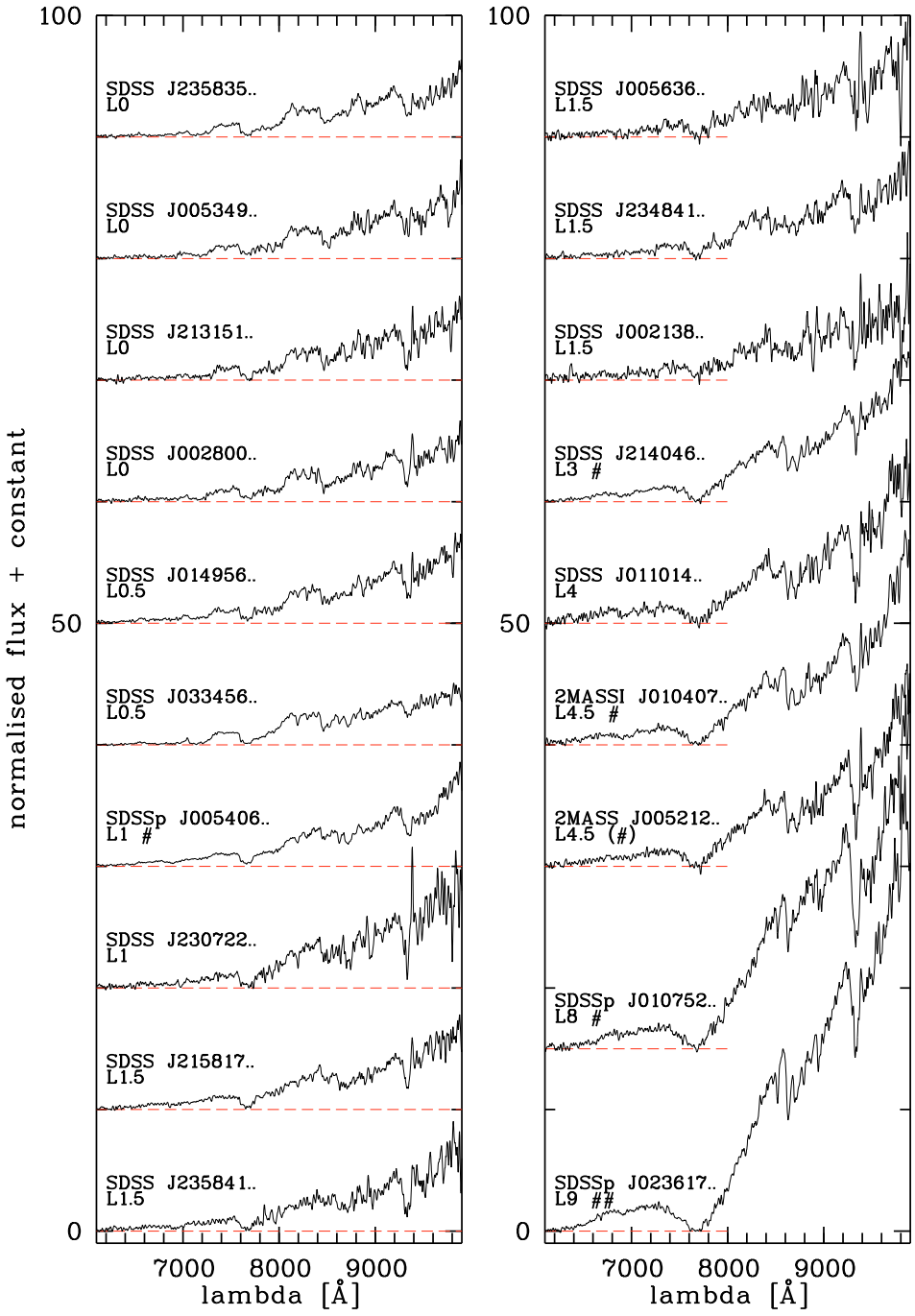

Fig. 3. VLT/FORS1 spectra of L dwarfs sorted by spectral type (*from top left to bottom right*). Comparison objects with previously known spectral types are marked by #. One comparison object with an available infrared but lacking optical spectral type is marked by (#), The object marked by ## has been re-classified by us as an L9 dwarf. All spectra are normalised at 7500 Å and smoothed with a running mean over 7 pixels.

three ultracool (>sdM7) subdwarfs. However, among the mid-M dwarfs, shown in more detail in Figs. 4 and 5, there are many objects which can be also fitted by the sdM7 template spectrum of LHS 377. This is due to our noisy spectra where the small but significant differences between the sdM7 (Gizis 1997) and the M 4.5–M 5.5 (Kirkpatrick et al. 1999) templates are hardly seen. The spectrum of SDSS J024958.88+010624.3 fits nearly perfectly with that of LHS 377, whereas two others (SDSS J215515.49+005128.0 and SDSS J231914.40+005615.9) are very close. We assign an alternative spectral type of sdM7 to these three targets. For four others (re-classified as sdM7:) we can still see a reasonable agreement with the spectrum of LHS 377. However, none of the sdM7-like spectra comes close to that of the sdM9.5 comparison object SSSPM J1013−1356 shown at the bottom of Fig. 5. Our earliest type M dwarf spectrum (SDSS J221911.35+010220.5; Fig. 4) fits reasonably well to that of LHS 320 (sdM2; Gizis 1997).

The spectrum of SDSS J021546.76+010019.2 is a peculiar one. On the red side, the continuum is as strong as that of an M5 dwarf (Fig. 4), whereas on the blue side the signal is much stronger but relatively featureless. We speculate that this may be caused by an unresolved white dwarf companion (for comparison see e.g. Raymond et al. 2003). It also looks like one of the mid-M extreme subdwarfs (esdM in the system of Gizis 1997),

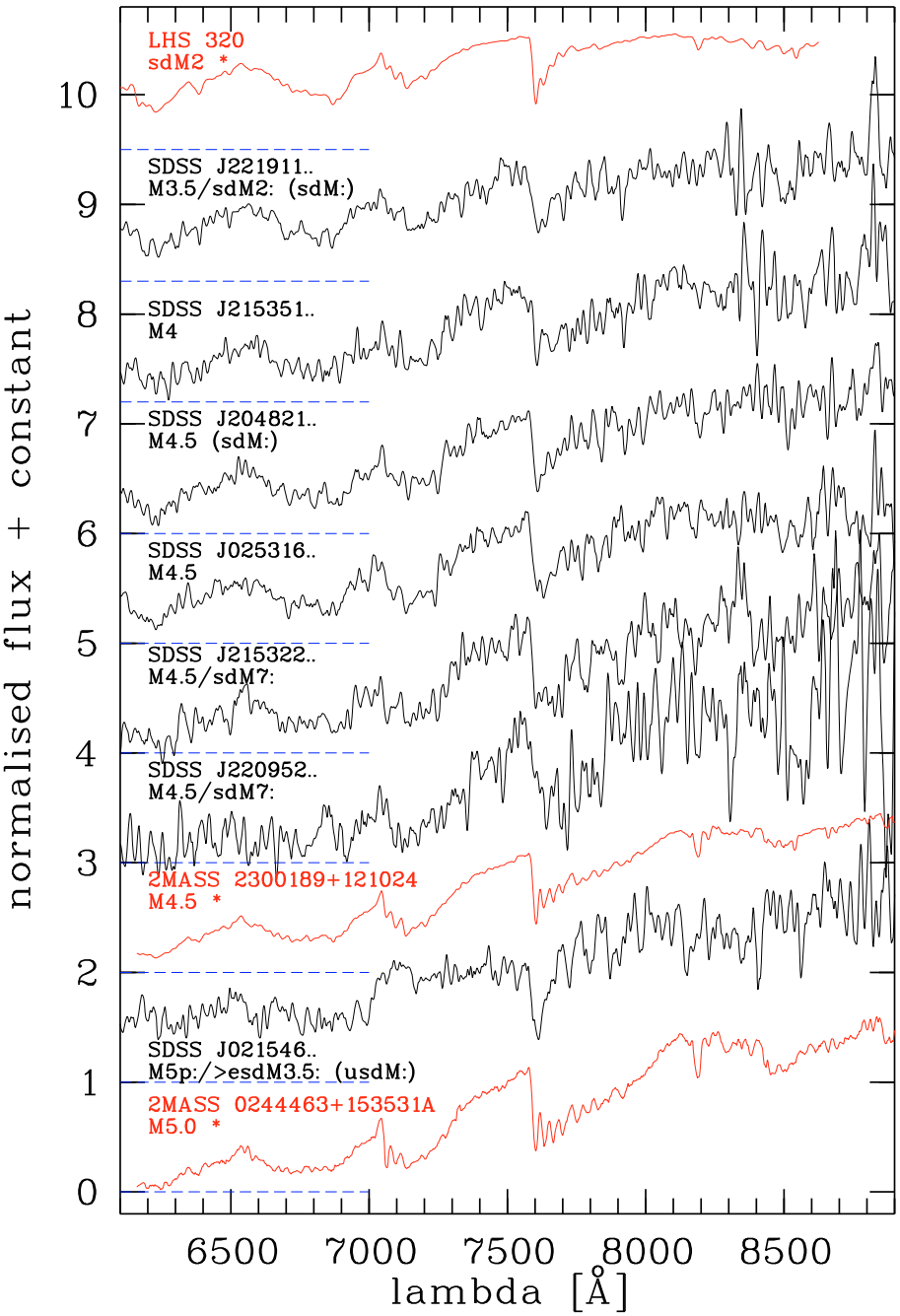

Fig. 4. VLT/FORS1 spectra of all objects initially classified as M 3.5–M 5p in comparison to Keck/LRIS spectra (marked by ∗) of known dwarfs and subdwarfs (Gizis 1997; Kirkpatrick et al. 1999). All spectra have been smoothed with a running mean over 7 pixels.

which we extracted from the aforementioned web page of Reid, while its continuum is as red as that of the known esdM8 object LEHPM 2–59 (see Fig. 7) but does not show either the characteristic absorption bands bluewards of 7000 Å or the strong KI doublet at 7665/7699 Å. Unfortunately, this peculiar spectrum has only a very low signal-to-noise ratio so that we assign an uncertain type of M5p:/>esdM3.5:. For all nine objects with an alternative subdwarf classification (Table 4), we estimate an uncertainty of at least one subdwarf type.

Although most of our spectra have only low signal-to-noise, which combined with the low resolution do not allow accurate measurements of the CaH and TiO5 indices used in the classification of M subdwarfs (Gizis 1997), we list the CaH1, CaH2, and CaH3 indices together with their errors in Table 3. Note that the accuracy of the CaH indices and of the TiO5 index in Gizis (1997) was ±0.02–0.04. This accuracy has been reached by us only in exceptional cases for all four indices. In the last column of Table 3 we give the $\zeta_{\rm TiO/CaH}$ defined by Lépine et al. (2007) for creating a new three-class (sdM, esdM, usdM) system instead of the two-class (sdM, esdM) system of Gizis (1997). The $\zeta_{\rm TiO/CaH}$ depends only on TiO5, CaH2, and CaH3. In case of our spectra, the latter three indices are generally better defined than the CaH1 index. We list the subdwarf class according to the $\zeta_{\rm TiO/CaH}$ values for all M-type objects in Table 4. There are seven moderately metal-poor subdwarf (sdM) candidates and one very low metallicity (usdM:) candidate, which is the already mentioned above esdM-like object SDSS J021546.76+010019.2, among the M dwarfs in our sample. Note that the esdM8.0

Table 3. Spectral indices measured for new HPM objects and comparison objects.

Name	PC3	err	TiO5	err	VOa	err	CaH1	err	CaH2	err	CaH3	err	$\zeta_{TiO/CaH}$
(1)	(2)	(3)	(4)	(5)	(6)	(7)	(8)	(9)	(10)	(11)	(12)	(13)	(14)
SDSS J002138.86+002605.8	2.35	0.23	1.35	0.49	2.10	0.46	3.42	3.86	1.07	0.41	2.29	0.93	–3.5
SDSS J002800.37+010252.0	2.35	0.11	0.43	0.07	2.17	0.19	4.51	4.59	0.37	0.07	0.52	0.06	0.77
SDSS J003435.32+004633.9	1.95	0.04	0.28	0.07	2.23	0.15	0.45	0.51	0.22	0.07	0.46	0.06	0.82
SDSS J003550.48+004631.3	1.68	0.10	0.05	0.09	2.40	0.22	0.66	0.48	0.17	0.09	0.58	0.06	1.15
SDSS J005349.11−011354.4	2.20	0.11	0.63	0.06	2.66	0.22	0.87	0.66	0.46	0.08	1.06	0.20	1.47
SDSS J005636.22−011131.9	4.25	0.67	0.98	0.24	2.46	0.35	0.97	0.45	0.12	0.14	0.58	0.24	0.03
SDSS J005837.48+004435.6	1.72	0.09	0.39	0.04	2.48	0.20	–74.	799.5	0.22	0.06	0.44	0.07	0.69
SDSS J010959.91−010156.3	1.03	0.11	1.08	0.11	2.17	0.22	1.11	0.22	1.03	0.12	1.12	0.12	0.48
SDSS J011014.30+010619.1	6.03	0.85	2.12	0.47	1.75	0.16	0.70	0.43	1.21	0.25	0.95	0.18	6.65
SDSS J011755.09+005220.0	1.17	0.05	0.55	0.03	2.24	0.15	1.05	0.30	0.26	0.06	0.62	0.05	0.60
SDSS J013415.85+001456.0	1.42	0.03	0.43	0.06	2.18	0.10	1.09	0.36	0.30	0.05	0.52	0.03	0.73
SDSS J014956.27+001647.8	2.45	0.11	0.55	0.14	2.48	0.15	1.27	0.18	0.56	0.10	0.69	0.12	0.94
SDSS J020508.04+002458.7	0.91	0.07	0.96	0.06	2.18	0.12	0.99	0.08	1.16	0.06	1.09	0.06	–0.2
SDSS J021546.76+010019.2	1.35	0.07	1.06	0.03	2.02	0.14	0.76	0.09	0.60	0.05	0.62	0.03	–0.1
SDSS J024958.88+010624.3	1.29	0.05	0.32	0.02	1.92	0.11	0.54	0.15	0.24	0.02	0.40	0.03	0.75
SDSS J025316.06+005157.1	1.01	0.04	0.36	0.02	2.12	0.13	0.78	0.04	0.40	0.03	0.81	0.04	1.27
SDSS J032129.20+003212.8	1.06	0.04	1.03	0.03	1.86	0.10	0.96	0.02	1.02	0.02	0.93	0.03	0.55
SDSS J033203.57+003658.0	1.15	0.05	0.45	0.04	2.33	0.15	0.73	0.13	0.33	0.03	0.84	0.05	1.03
SDSS J033456.32+010618.7	2.56	0.06	0.10	0.03	2.00	0.09	0.75	0.60	0.21	0.03	0.25	0.03	0.91
SDSS J204821.28−004734.1	1.14	0.05	0.62	0.04	2.17	0.07	1.40	0.14	0.53	0.04	0.66	0.04	0.72
SDSS J213151.87−001432.4	2.14	0.12	0.97	0.36	2.64	0.28	–3.5	–4.39	0.39	0.21	0.81	0.26	0.06
SDSS J215322.18−004553.9	1.09	0.07	0.31	0.04	1.93	0.12	1.21	0.46	0.48	0.03	0.68	0.06	1.27
SDSS J215351.20+010120.3	1.02	0.04	0.38	0.04	1.89	0.12	0.91	0.26	0.37	0.07	0.55	0.09	0.86
SDSS J215515.49+005128.0	1.32	0.06	0.24	0.02	1.86	0.13	0.73	0.19	0.33	0.05	0.53	0.04	1.00
SDSS J215817.69+000300.3	2.78	0.13	0.89	0.08	2.11	0.10	0.51	0.37	0.74	0.07	0.71	0.07	0.34
SDSS J215934.25+005308.5	1.92	0.10	0.36	0.09	2.49	0.19	1.37	0.32	0.36	0.08	0.57	0.12	0.90
SDSS J220952.49+003325.2	1.10	0.12	0.46	0.10	1.99	0.30	1.21	0.50	0.69	0.10	0.53	0.11	1.08
SDSS J221911.35+010220.5	1.16	0.06	0.74	0.09	2.09	0.12	0.69	0.09	0.52	0.05	0.85	0.04	0.68
SDSS J222939.14+010405.5	0.93	0.04	1.04	0.06	1.80	0.10	0.83	0.08	1.04	0.05	1.00	0.07	0.35
SDSS J225903.29−004154.2	2.06	0.09	0.12	0.03	2.43	0.12	1.08	0.42	0.09	0.06	0.36	0.08	0.89
SDSS J230722.58−005746.6	2.64	0.15	0.59	0.09	2.44	0.40	2.66	1.77	0.39	0.07	0.11	0.04	0.43
SDSS J231407.82+004908.2	1.95	0.09	0.26	0.07	2.34	0.11	1.10	0.29	0.31	0.06	0.40	0.09	0.86
SDSS J231914.40+005615.9	1.34	0.09	0.37	0.07	1.97	0.14	1.18	0.33	0.40	0.06	0.57	0.05	0.92
SDSS J232935.99−011215.3	1.99	0.09	0.06	0.05	2.10	0.13	–0.5	0.35	0.25	0.07	0.55	0.12	1.17
SDSS J234841.38−004022.1	3.03	0.19	1.00	0.10	2.13	0.19	0.22	0.24	0.78	0.12	0.69	0.07	0.00
SDSS J235826.48+003226.9	1.72	0.08	0.33	0.06	2.34	0.13	0.82	0.35	0.16	0.05	0.67	0.10	0.85
SDSS J235835.45−000909.5	2.17	0.10	0.17	0.03	2.28	0.12	1.35	0.53	0.44	0.03	0.71	0.04	1.51
SDSS J235841.98+000622.0	2.82	0.23	0.75	0.17	1.96	0.26	1.00	0.27	0.65	0.09	0.74	0.05	0.70
comparison L dwarfs in S82:													
2MASS J00521232+0012172	4.79	0.55	1.86	0.21	1.78	0.15	1.33	0.33	1.25	0.22	1.19	0.20	3.22
SDSSp J005406.55−003101.8	2.66	0.07	0.96	0.04	2.15	0.09	0.72	0.08	0.54	0.04	0.68	0.06	0.09
2MASSI J0104075−005328	5.65	0.44	0.85	0.07	1.66	0.11	0.99	0.20	0.61	0.05	0.53	0.04	0.27
SDSSp J010752.33+004156.1	7.30	0.72	1.00	0.05	2.09	0.19	2.29	2.48	1.03	0.08	0.92	0.06	0.03
SDSSp J023617.93+004855.0	10.41	0.61	1.21	0.08	2.14	0.18	0.71	0.22	0.94	0.05	0.96	0.05	10.4
SDSS J214046.55+011259.7	4.02	0.31	1.11	0.06	1.85	0.14	0.84	0.25	0.84	0.06	0.70	0.05	–0.4
comparison cool subdwarfs:													
SDSS J125637.12−022452.4	3.60	0.12	0.27	0.01	1.82	0.07	0.32	0.05	0.15	0.01	0.19	0.02	0.71
LSR 1610−0040	1.60	0.02	0.37	0.02	2.09	0.01	0.75	0.04	0.29	0.01	0.52	0.02	0.80
SSSPM J1013−1356	1.69	0.02	0.36	0.02	2.08	0.02	0.37	0.03	0.12	0.01	0.22	0.01	0.63
LEHPM 2–59	1.34	0.02	0.84	0.05	2.11	0.03	0.37	0.02	0.20	0.01	0.29	0.01	0.17
comparison CWD:													
SDSSp J133739.40+000142.8	0.71	0.04	0.93	0.03	1.92	0.08	1.00	0.03	1.16	0.03	1.04	0.02	–0.3

comparison object LEHPM 2–59 is also an usdM according to the new scheme of Lépine et al. (2007). The two new M 8.0 and M 8.5 dwarfs with an sdM: indication from their $\zeta_{TiO/CaH}$, SDSS J003435.32+004633.9 and SDSS J005837.48+004435.6, show spectra clearly distinctive from both late-subdwarf (sdM9.5 and esdM8.0) comparison spectra (bottom of Fig. 2).

With 9 out of 13 objects with an alternative subdwarf classification and two more objects with a hint of a subdwarf nature obtained from their $\zeta_{TiO/CaH}$ it seems possible that all the mid-M dwarfs are in fact subdwarfs. However, there is one object, SDSS J013415.85+001456.0, classified as M 5.5 and possibly being an sdM: according to its $\zeta_{TiO/CaH}$, which has a spectrum

Table 4. Spectral types, distances and tangential velocities of new HPM objects and comparison objects.

Name abbreviated (1)	SpT PC3 (2)	Err (3)	SpT TiO5 (4)	Err (5)	SpT VOa (6)	Err (7)	SpT Ind (8)	SpT Comp (9)	SpT Adopted (10)	sd ? $\zeta_{TiO/CaH}$ (11)	d_{spec} [pc] (12)	v_{tan} [km s^{-1}] (13)
SDSS J002138..	M9.7	0.5	L3.9	2.8	L2.0	3.3	L1.9	L1.5	L1.5		112	97
SDSS J002800..	M9.7	0.2	M8.7	0.4	L1.4	1.3	M9.9	L0.5	L0.0		151	119
SDSS J003435..	M8.4	0.2	M7.8	0.4	M7.1	1.6	M7.8	M8.5	M8.0	sdM:	197	134
SDSS J003550..	M7.3	0.5	M7.7	1.0	M9.0	2.3	M8.0	M7.5	M8.0		266	202
SDSS J005349..	M9.3	0.3	M9.8	0.4	M8.0	1.6	M9.9	L0.5	L0.0		149	102
SDSS J005636..	L2.7	0.5	L1.8	1.4	M9.4	2.5	L1.3	L1.5	L1.5		119	94
SDSS J005837..	M7.5	0.4	M8.5	0.2	M9.3	1.4	M8.4	M9.0	M8.5	sdM:	182	290
SDSS J010959..	M3.2	0.8	<M0	1.1	M6.5	2.3		CWD	CWD		165*	221
SDSS J011014..	L4.0	0.5	L8.3	2.7	L4.4	1.1	L4.2	L3.5	L4.0		64	166
SDSS J011755..	M4.3	0.3	M2.2	0.3	M7.3	1.6	M4.6	M5.0	M5.0/sdM7:	sdM:	920/625	(762/518)†
SDSS J013415..	M5.9	0.2	M3.6	0.6	M6.7	1.0	M5.4	M6.0	M5.5	sdM:	612	381
SDSS J014956..	M9.9	0.2	M9.4	0.8	M9.3	1.1	M9.5	L1.0	L0.5		118	99
SDSS J020508..	M2.3	0.5	<M0	0.6	M6.6	1.3		CWD	CWD		118*	104
SDSS J021546..	M5.4	0.5	<M0	0.3	M5.0	1.5		esdM:	M5p:/>esdM3.5:	usdM:	1068/<1138	869/<926
SDSS J024958..	M5.0	0.3	M4.7	0.2	M3.9	1.2	M4.5	M5.5	M5.0/sdM7	sdM:	886/602	617/419
SDSS J025316..	M3.1	0.3	M4.3	0.3	M6.0	1.3	M4.5	M4.5	M4.5		1387	1050
SDSS J032129..	M3.4	0.3	<M0	0.3	M3.2	1.0		CWD	CWD		129*	110
SDSS J033203..	M4.1	0.4	M3.4	0.5	M8.3	1.6	M5.2	M5.5	M5.5/sdM7:		872/719	(678/559)†
SDSS J033456..	L1.3	0.1	M6.8	0.2	L2.7	0.6	L0.3	L0.5	L0.5		103	197
SDSS J204821..	M4.0	0.4	M1.5	0.4	M6.5	0.7	M4.0	M4.5	M4.5	sdM:	1109	(2119)†
SDSS J213151..	M9.1	0.4	L1.7	2.1	M8.2	2.0	M9.7	L0.5	L0.0		141	101
SDSS J215322..	M3.7	0.5	M4.9	0.5	M4.0	1.3	M4.2	M5.0	M4.5/sdM7:		1360/704	(1817/941)†
SDSS J215351..	M3.2	0.3	M4.1	0.4	M3.6	1.2	M4.0	M4.0	M4.0		1626	(1185)†
SDSS J215515..	M5.2	0.4	M5.6	0.2	M3.2	1.3	M4.7	M5.5	M5.0/sdM7		862/585	(604/410)†
SDSS J215817..	L1.5	0.1	L1.3	0.4	L1.9	0.7	L1.6	L1.0	L1.5		106	74
SDSS J215934..	M8.3	0.4	M8.3	0.5	M9.2	1.4	M8.6	L0.5	M9.5		206	193
SDSS J220952..	M3.7	0.8	M3.3	1.0	M4.7	3.1	M3.9	M5.5	M4.5/sdM7:		1285/665	(920/476)†
SDSS J221911..	M4.2	0.4	M0.2	1.0	M5.7	1.3	M3.4	M4.0	M3.5/sdM2:	sdM:	2548/1910	(2454/1839)†
SDSS J222939..	M2.5	0.3	<M0	0.7	M2.7	1.1		CWD	CWD		135*	115
SDSS J225903..	M8.9	0.3	M6.9	0.2	M9.3	1.2	M8.4	M8.0	M8.0		265	(319)†
SDSS J230722..	L1.3	0.1	M9.6	0.5	M9.6	2.8	L0.2	L2.0	L1.0		136	91
SDSS J231407..	M8.5	0.3	M7.7	0.4	M8.3	1.2	M8.2	M8.0	M8.0		243	202
SDSS J231914..	M5.4	0.5	M4.2	0.8	M4.4	1.5	M4.7	M6.0	M5.5/sdM7		949/782	(2304/1899)†
SDSS J232935..	M8.6	0.3	M6.6	0.3	M5.8	1.4	M7.0	M8.0	M7.5		281	194
SDSS J234841..	L1.7	0.2	L1.9	0.6	L1.7	1.3	L1.8	L1.5	L1.5		112	91
SDSS J235826..	M7.5	0.4	M8.1	0.3	M8.4	1.3	M8.0	M7.5	M8.0		283	242
SDSS J235835..	M9.2	0.3	M7.2	0.2	L0.7	0.9	M9.0	L0.5	L0.0		112	132
SDSS J235841..	L1.5	0.2	L0.5	1.0	L2.9	1.8	L1.6	L1.0	L1.5		122	109
comparison L												
2MASS J005212..	L3.1	0.4	L6.8	1.2	L4.2	1.1	L4.7	L4.5	L4.5		53	62
SDSSp J005406..	L1.4	0.1	L1.6	0.2	L1.6	0.6	L1.5		L1.0		55	77
2MASSI J010407..	L3.7	0.3	L1.0	0.4	L5.1	0.8	L3.3		L4.5		51	110
SDSSp J010752..	L4.7	0.4	L1.9	0.3	L2.0	1.3			L8.0		17	51
SDSSp J023617..	L5.8	0.1	L3.1	0.4	L1.7	1.3		L9.0	L9.0		18	17
SDSS J214046..	L2.5	0.2	L2.5	0.3	L3.7	1.0	L2.9		L3.0		54	56
comparison sd												
SDSS J125637..	L2.2	0.1	M7.8	0.1	L3.9	0.5			sdL4:	sdL	120[1]	353[1]
LSR 1610−0040	M6.9	0.1	M4.2	0.2	M5.7	0.2			M6p/sdM	sdM	32[2]	221[2]
SSSPM J1013..	M7.3	0.1	M8.3	0.1	L2.1	0.1			sdM9.5	sdM	50[3]	244[3]
LEHPM 2–59	M5.4	0.1	L1.0	0.3	M5.9	0.3			esdM8	usdM	66[4]	233[4]
comparison CWD												
SDSSp J133739..	M0.6	0.3	<M0	0.4	M3.9	0.8			CWD		20–54[5]	17–46[5]

Notes: [1] – Sivarani et al. (2004); Burgasser et al. (2007); [2] – according to Dahn et al. (2008); [3] – Scholz et al. (2004a); [4] – Pokorny et al. (2004), Burgasser & Kirkpatrick (2006); [5] – Harris et al. (2001). Distances in Col. (12) marked by * were derived assuming an absolute magnitude of $M_i = 15.9$; uncertainties in distances and tangential velocities are ~23% for M 7–L 9 dwarfs and ~46% for new CWDs and M 3–M 6 dwarfs (including alternative subdwarf types) (see text). Objects with tangential velocities in Col. (13) marked by † have uncertain proper motions (see Table 1). Their tangential velocities (putted in parentheses) have therefore an additional uncertainty, i.e. they may be overestimated by an unknown factor.

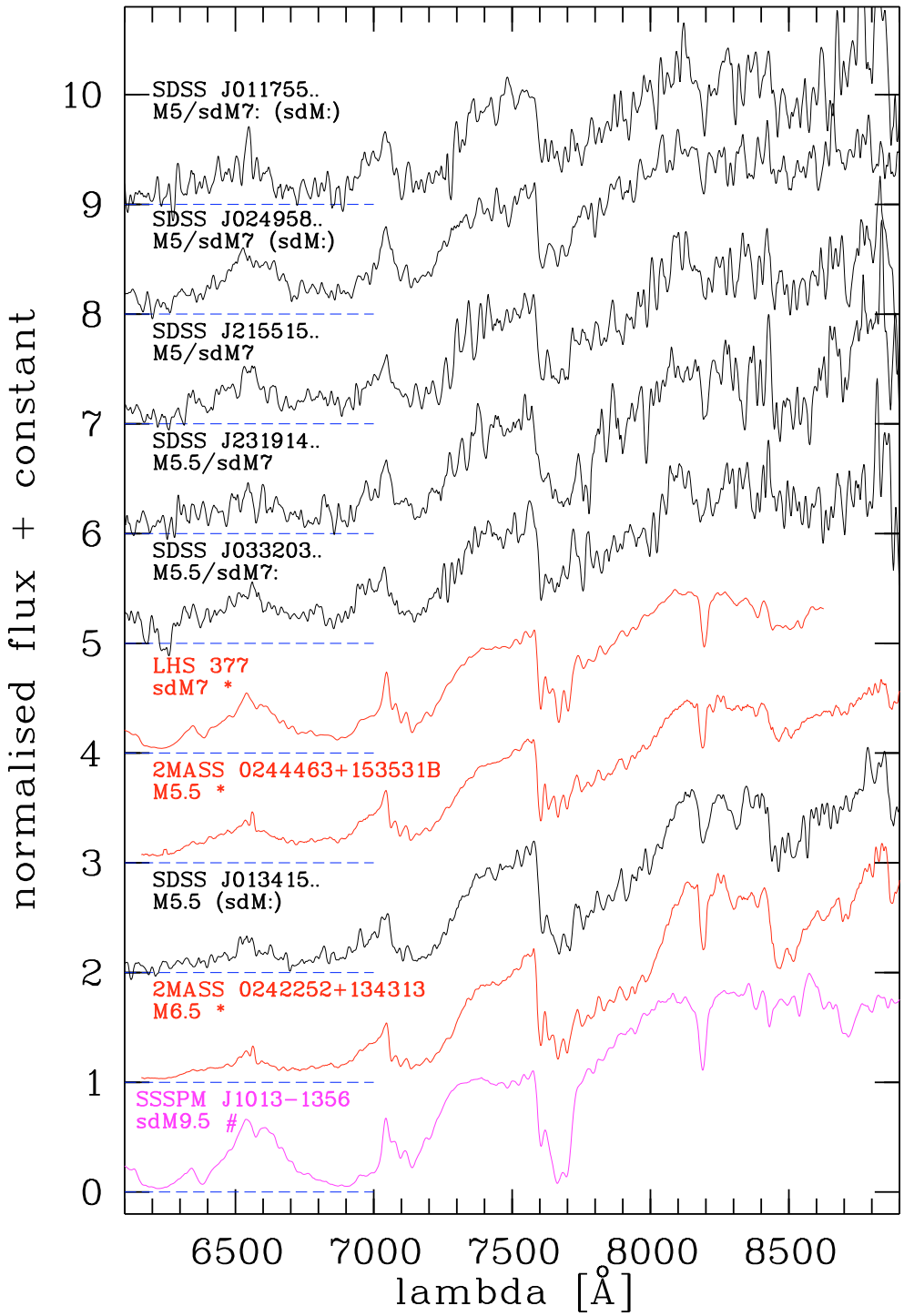

Fig. 5. Same as Fig. 4 for all objects initially classified as M 5–5.5. Also shown for comparison is the VLT/FORS1 spectrum of SSSPM J1013−1356.

clearly typical of a normal mid-M dwarf (Fig. 5). In the spectrum of SDSS J011755.09+005220.0, reclassified as sdM7: and having an sdM: flag from its $\zeta_{\rm TiO/CaH}$, we see an Hα line in emission (top of Fig. 5), which is usually not observed in subdwarfs and would support its initial classification as a normal M 5 dwarf.

3.4. Cool white dwarfs

Four new HPM objects (all with $i-z < +0.4$) show featureless spectra similar to that of the known cool white dwarf SDSSp J133739.40+000142.8 (upper left part of Fig. 2). Compared to the latter the new objects show a less pronounced blue continuum in their spectra. However, they are much bluer than the earliest M (sub)dwarfs in our sample, and their *gr* magnitudes are well measured. We list the additional photometry for those four objects in Table 5 together with that of the only M (sub)dwarf with well-measured *gr* magnitudes, SDSS J221911.35+010220.5 (M3.5/sdM2:), which is the fifth object with $i-z < +0.4$ similar to the four CWDs but with an uncertain proper motion (see Fig. 1). The *u* magnitudes given in Table 5

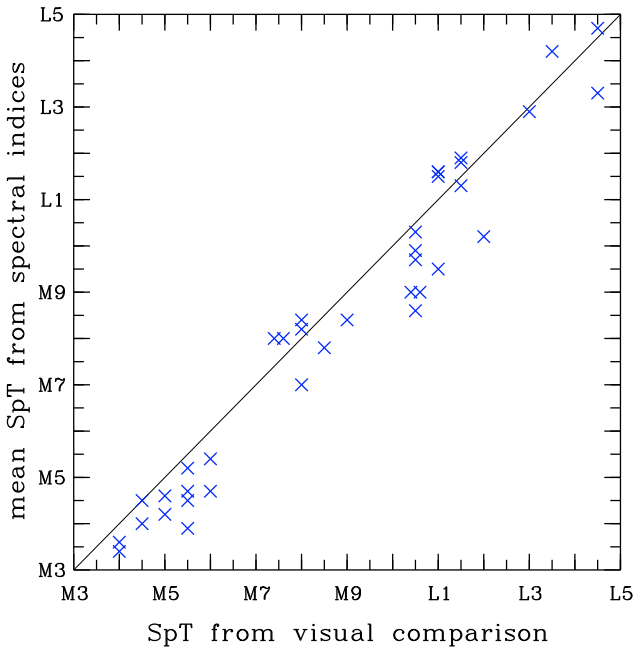

Fig. 6. Mean spectral types obtained from spectral indices vs. spectral types obtained from visual comparison with M and L dwarf template spectra. All our targets (except the CWDs and the peculiar object SDSS J021546.76+010019.2) are shown together with the comparison L dwarfs (except two late-L dwarfs). For four objects, the visual spectral types were shifted by ±0.1 subclasses for better visibility. The line indicates consistence of spectral types.

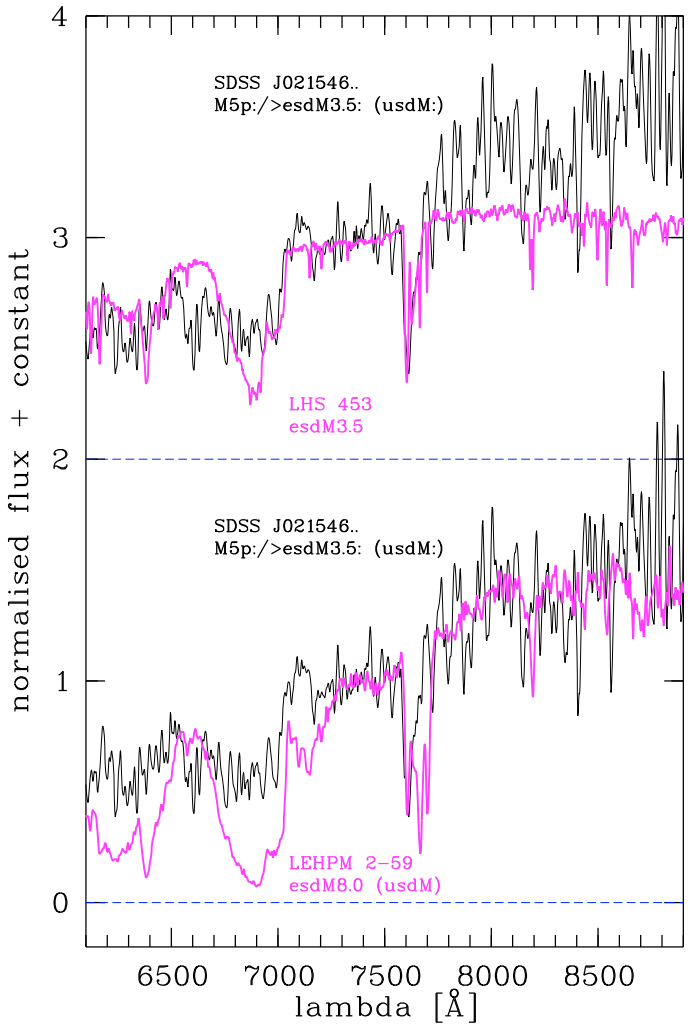

Fig. 7. Spectrum of the peculiar M5p:/>esdM3.5: object SDSS J021546.76+010019.2 (usdM: according to the new system of Lépine et al. 2007) compared to that of the comparison esdM8.0 (usdM) object LEHPM 2-59 (both spectra taken with VLT/FORS1) and to the Keck/LRIS spectrum of LHS 453 (esdM3.5; Gizis 1997) from Neill Reid's webpage. The comparison spectra (thin lines) were not smoothed, whereas the noisy spectrum of SDSS J021546.76+010019.2 was smoothed with a running mean over 7 pixels (thick line).

are lower limits, since all our faint ($i > 21$) objects were only partly detected in that passband (the number of detections in gr and in u are given in the last two columns, respectively). As one can see, not only is the spectrum of SDSS J221911.35+010220.5 clearly distinguished but also its $g - r$ and $r - i$ colours are much redder than those of the CWDs.

Our spectra cover a smaller wavelength interval than used for the classification of other CWDs discovered in the SDSS (e.g. Gates et al. 2004; Harris et al. 2008), and more spectroscopic data (and model atmosphere fitting) are needed to better characterise our objects. However, the accurately measured large proper motions and colours (Tables 1, 5) of the four objects with featureless spectra support their classification as CWDs. Their $g - r$, $r - i$ and $i - z$ colours are similar to those of other CWDs with mild collision-induced absorption (CIA) described by Harris et al. (2008). On the other hand, the only comparison CWD observed by us, SDSSp J133739.40+000142.8, is typical of CWDs with strong CIA suppression and temperatures below 4000 K (Gates et al. 2004). Our new CWDs are probably warmer.

4. Distance estimates and kinematics

Spectroscopic distances of all M and L dwarfs and their resulting tangential velocities (Table 4) were derived using absolute magnitudes M_z of L dwarfs later than L2 given by Hawley et al. (2002) and the revised data with updated SDSS colours for M 0 to L 2 dwarfs from West et al. (2005). The values for half-step spectral types were determined by linear interpolation between the neighbouring absolute magnitudes for integer spectral types.

For an estimate of the expected uncertainties in the distances and tangential velocities, we have made a conservative assumption of 0.5 mag accuracy in the absolute magnitudes of all late-M and L dwarfs. This includes an uncertainty of one spectral type corresponding to about 0.3–0.4 mag differences in M_z. For M 3–M 6 dwarfs, the uncertainty of one spectral type corresponds to 0.8–1.2 mag differences in M_z. Therefore, we use a 1.0 mag accuracy in the absolute magnitudes of M 3–M 6 dwarfs for our distance calculation. Note that for all M and L dwarfs the uncertainties in colours are relatively small (0.1–0.2 mag), and that the changes in $z - J$ in the recent paper by West et al. (2008) compared to those in West et al. (2005) are also of that order. Our assumed uncertainties in the absolute magnitudes lead to 23% and 46% distance (and tangential velocity) errors, respectively for M 7–L 9 and M 3–M 6 dwarfs. The errors in the proper motions have a much smaller effect on the uncertainties of the tangential velocities and were neglected. However, for objects with uncertain proper motions marked in Tables 1 and 4 this is not the case. Their tangential velocities may be overestimated by an unknown factor corresponding to the possibly overestimated proper motions.

Table 5. Additional *ugr* photometry of objects with well-measured *gr* magnitudes (for *iz* magnitudes see Table 1).

Name from SDSS DR6 (SDSS J...)	SpT	Mean u [mag]	Mean g [mag]	Mean r [mag]	$u-g$ [mag]	$g-r$ [mag]	$r-i$ [mag]	$i-z$ [mag]	N_{gr}	N_u
(1)	(2)	(3)	(4)	(5)	(6)	(7)	(8)	(9)	(10)	(11)
010959.91−010156.3	CWD	>23.987	23.420	22.346	>+0.567	+1.074	+0.361	+0.261	23	14
		±0.275	±0.080	±0.120	±0.286	±0.144	±0.137	±0.135		
020508.04+002458.7	CWD	>24.114	22.216	21.532	>+1.899	+0.684	+0.276	+0.045	44	35
		±0.232	±0.020	±0.013	±0.233	±0.024	±0.026	±0.076		
032129.20+003212.8	CWD	>24.684	22.663	21.765	>+2.021	+0.899	+0.319	+0.141	21	15
		±0.362	±0.054	±0.021	±0.366	±0.060	±0.033	±0.096		
222939.14+010405.5	CWD	>24.461	22.609	21.892	>+1.851	+0.718	+0.345	−0.341	15	12
		±0.443	±0.045	±0.040	±0.445	±0.060	±0.067	±0.178		
221911.35+010220.5	M3.5/sdM2: (sdM:)	>24.976	24.267	22.654	>+0.709	+1.613	+0.988	+0.325	9	4
		±0.660	±0.273	±0.098	±0.714	±0.290	±0.103	±0.144		

For a second distance estimate of the nine mid-M dwarfs with alternatively adopted subdwarf types, we have used the trigonometric parallaxes of the corresponding comparison objects, LHS 453 and LHS 377 (10.3 ± 0.9 mas and 28.4 ± 0.8 mas, respectively from Monet et al. 1992), and LHS 320 (25.8 ± 3.6 mas from van Altena et al. 1995). All three comparison objects have been measured in the SDSS. We have used the z magnitudes from SDSS DR6 (Adelman-McCarthy et al. 2008) of 12.878 ± 0.006 and 14.673 ± 0.006, respectively for LHS 320 and LHS 377. For LHS 453, we used the SDSS DR7 (Abazajian et al. 2008) z magnitude of 15.897 ± 0.007. The absolute magnitudes M_z are 9.94 ± 0.30, 10.96 ± 0.19, and 11.94 ± 0.06, respectively for LHS 320 (sdM2), LHS 453 (esdM3.5), and LHS 377 (sdM7). For the resulting alternative distances and tangential velocities of our targets (Table 4) we again estimate errors of about 46% based on our assumed greater uncertainty of 1 mag in the absolute magnitudes which is dominated by the expected uncertainty of more than one type in our subdwarf classification.

Since all newly discovered L dwarfs have spectral types between L0 and L4.5 we compare their measured mean i magnitudes and proper motions as well as the determined spectroscopic distances and tangential velocities with the data of all previously known L 0–L 4.5 dwarfs in S82 in Fig. 8. As one can see, the known early-L dwarfs are mostly brighter and have on average smaller proper motions. Consequently, the new L dwarfs have larger distances (between 60 and 150 pc) and tangential velocities (70 to 200 km s^{-1}), which are typical of the Galactic thick disk and halo. None of the new L dwarfs has been marked as an uncertain proper motion object († in Tables 1 and 4), so that their relatively high velocities seem to be reliable. There are two new L dwarfs (SDSS J005636.22−011131.9 and SDSS J235841.98+000622.0) with formal proper motion errors larger than ±25 mas/yr, but their tangential velocities are only moderately large (∼100 km s^{-1}). With this study we have considerably increased the number of high-velocity L dwarfs compared to follow-up proper motion determinations of large numbers of L dwarfs (Schmidt et al. 2007; Faherty et al. 2008) discovered previously in large area (all-sky) surveys. Among a total of more than 400 late-M and L dwarfs investigated, the latter two studies include only 10 normal L dwarfs with $v_{\rm tan} > 100$ km s^{-1}, whereas we have discovered 7 in a much smaller sky area. This underlines that a HPM survey which goes to fainter magnitudes is a powerful tool to detect those "fast" L dwarfs.

The spectroscopic distance of the L 8 dwarf SDSSp J010752.33+004156.1 (17 ± 4 pc) agrees very well with its trigonometric parallax of 64.13 ± 4.51 mas measured by Vrba et al. (2004). This agreement supports our re-classification of the previously known L 6 dwarf SDSSp J023617.93+004855.0 as an

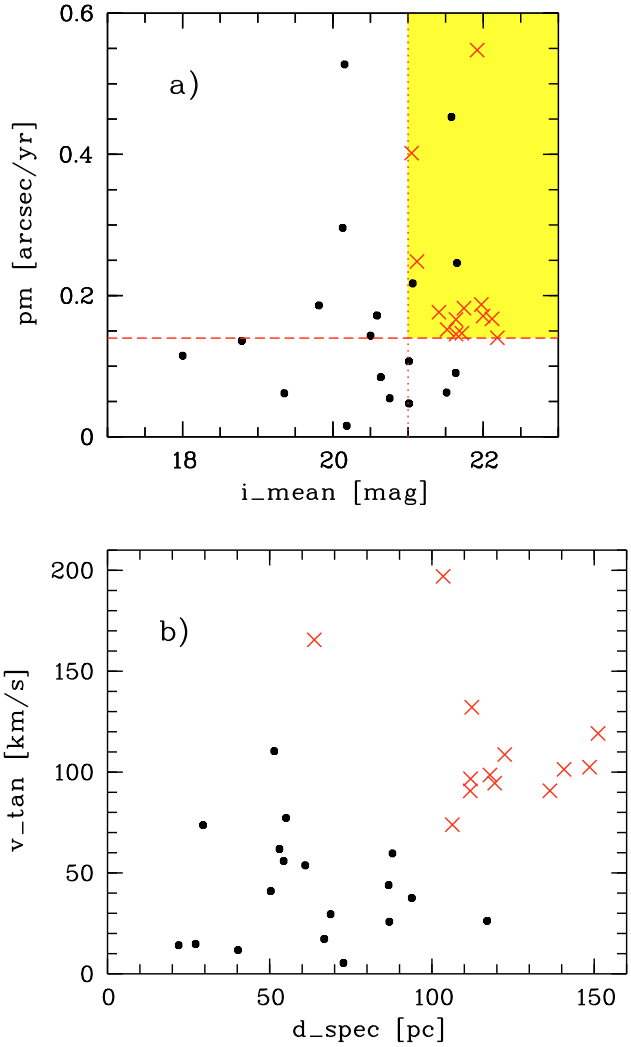

Fig. 8. a) Mean i magnitudes and proper motions of all previously known (dots) and new (crosses) L 0–L 4.5 dwarfs in S82. The area *right of the dotted line* and above the dashed line marks the selection criteria of our proper motion survey; **b)** spectroscopic distances and tangential velocities of previously known (dots) and new (crosses) L 0–L 4.5 dwarfs in S82.

L 9 dwarf (Sect. 3.2). An alternative earlier (L5.5) classification of SDSSp J010752.33+004156.1 while accepting the L6 type of SDSSp J023617.93+004855.0 would lead to a much larger spectroscopic distance (27 ± 6 pc) of SDSSp J010752.33+004156.1, i.e. nearly two times larger than the trigonometric distance estimate.

Even larger distances (180 to 280 pc) and corresponding tangential velocities (130 to 320 km s^{-1}) have been estimated for the eight late-M dwarfs in our sample. The highest velocity corresponds to the only uncertain proper motion object (SDSS J225903.29−004154.2) among them. Three objects (SDSS J215934.25+005308.5, SDSS J232935.99−011215.3, SDSS J235826.48+003226.9) have proper motion errors larger than ±25 mas/yr, and two others are mentioned as sdM candidates. Despite these uncertainties, the late-M dwarfs probably also belong to the thick disk/halo populations. None of the seven late-M dwarfs with tangential velocities of the order of 200 km s^{-1} and more, similar to those of the three comparison ultracool subdwarfs (Table 4), show obvious low-metallicity indications in their spectra, i.e. they do not resemble the spectra of any of these ultracool subdwarfs (Fig. 2). According to our findings, there is apparently a population of high-velocity normal late-M dwarfs in addition to that of ultracool subdwarfs. Note that Faherty et al. (2008) have found only three normal late-M dwarfs with tangential velocities exceeding 100 km s^{-1} among >250 previously classified M 7–M 9.5 dwarfs lacking proper motions, whereas Schmidt et al. (2007) have failed to find any among about 80 investigated M 7–M 9.5 dwarfs within 20 pc.

The spectroscopic distances of the 13 mid-M dwarfs range from about 600 to 2500 pc, and their tangential velocities lie between about 400 and 2500 km s^{-1}, if the proper motions are correct. However, seven out of nine objects with tangential velocities above 700 km s^{-1} are uncertain proper motion objects (Table 4) so that we consider these very high velocities as highly uncertain, too. The majority of the mid-M dwarfs have an alternative subdwarf classification, and we cannot exclude that all the mid-M dwarfs with rather noisy spectra are in fact subdwarfs. The subdwarf classification reduces our extreme distance and tangential velocity estimates by up to about 50% (see also Scholz et al. 2005). Among the four mid-M (sub)dwarfs not marked as uncertain proper motion objects, there are the M5p:/>esdM3.5: object SDSS J021546.76+010019.2 and the M 4.5 dwarf SDSS J025316.06+005157.1 with velocities of the order of 1000 km s^{-1}. Their proper motion errors are larger than ±25 mas/yr and amount to about 20–25% uncertainty in their proper motion values. Our assumed total uncertainty of 46% in their tangential velocities, which is dominated by the uncertain spectral types and absolute magnitudes, is still consistent with a velocity below the local Galactic escape velocity (Smith et al. 2007). For many of the 13 objects classified as mid-M dwarfs our proper motions are probably overestimated. But those for which the proper motion measurement is approximately correct are likely Galactic halo members.

As already mentioned in Sect. 3.4, our four new CWDs have SDSS colours consistent with the mild-CIA class of CWDs described in Harris et al. (2008). In order to obtain distance estimates for our targets we have used two of the objects discovered by Harris et al. (2008), SDSS J0310−01 and SDSS J1632+24 (=LP386–28; Luyten 1979b) for comparison. The latter two objects have according to the i magnitudes and distances given by Harris et al. (19.87, 40–99 pc and 18.51, 21–52 pc, respectively for SDSS J0310−01 and SDSS J1632+24) very similar absolute magnitudes of M_i = 15.9 with an uncertainty of 1.0 mag. We have assigned this mean absolute magnitude to all our CWDs and determined distances of between about 120 and 170 pc. The assumed uncertainty of 1.0 mag in the absolute magnitudes corresponds to 46% errors in the distances and tangential velocities of the new CWDs. The proper motion errors of all new CWDs are small so we have neglected their effect on the uncertainties of the computed tangential velocities. Three of the resulting tangential velocities lie between 100 and 120 km s^{-1} and indicate thick disk or halo membership, whereas the faintest CWD, SDSS J010959.91−010156.3, has a higher tangential velocity of about 220 km s^{-1} which qualifies this object as a likely halo member.

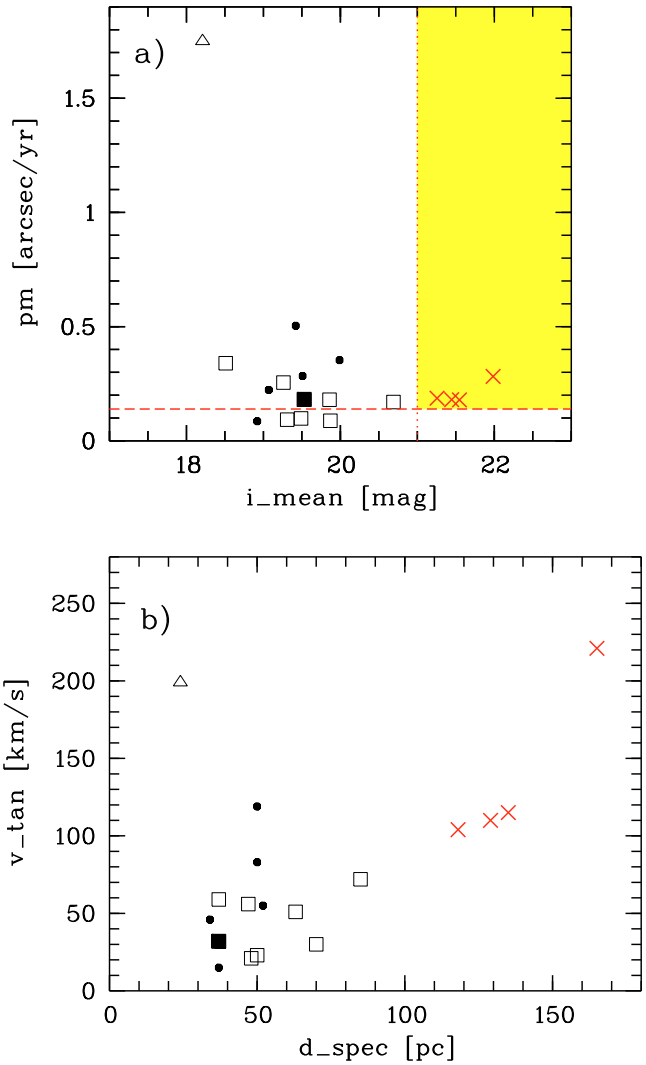

Fig. 9. a) Mean i magnitudes and proper motions of new CWDs discovered in S82 (crosses) compared to those of other spectroscopically confirmed CWDs discovered from SDSS: filled square – Harris et al. (2001), dots – Gates et al. (2004), open squares – Harris et al. (2008), triangle – Hall et al. (2008). The area *right of the dotted line* and above the dashed line marks the selection criteria of our S82 proper motion survey; **b)** spectroscopic distances and tangential velocities of the new (crosses) and previously discovered SDSS CWDs (symbols as in a) with same objects shown). Mean values of the different estimates for all previously known CWDs were used here.

Compared to spectroscopically confirmed CWDs formerly detected in SDSS data (Harris et al. 2001; Gates et al 2004; Harris et al. 2008; Hall et al. 2008) our new CWDs are generally fainter by about 2 mag but still have similarly large (and well-measured) proper motions (Fig. 9a). There is an important

difference between the last two figures: Whereas the comparison early-L dwarfs in Fig. 8 represent the previously known census in the S82 area, the comparison CWDs in Fig. 9 have been detected in the whole SDSS, i.e. in a sky area about 40 times larger than our survey area. Since we assume our new CWDs have the same mean absolute magnitudes as the two comparison objects from Harris et al. (2008; see above), the new objects are consequently at much larger distances and have exclusively thick disk and halo kinematics, whereas most of the previous SDSS discoveries have lower velocities typical of the thin disk population (Fig. 9b). However, we cannot exclude that some of our new CWDs have fainter absolute magnitudes. Trigonometric parallax measurements are needed to clarify this issue.

5. Conclusions

1. We have carried out a HPM survey of faint objects in S82 using their individual epoch positions from 1998 to 2004. The 38 faintest HPM objects ($i > 21$, $\mu > 0.14$ arcsec/yr) have been selected (together with some comparison objects) for our spectroscopic follow-up observations. Very recently, in an independent attempt to find moving sources in S82, Lang et al. (2008) used a method of fitting a model of a moving point source to all S82 imaging data. Their initial candidate list was selected from the S82 "Co-add catalog" (Annis et al., in prep.) aiming at the detection of HPM objects that are too faint to detect at any individual epoch. Among their 19 HPM brown dwarf candidates (with proper motions between 0.07 and 0.65 arcsec/yr) there are 10 previously known objects (nine L dwarfs and one T dwarf), which were all detected in our survey, too. Among the remaining objects of Lang et al. there are only four with proper motions $\mu > 0.14$ arcsec/yr. Two of the latter (SDSS J011014.30+010619.1 and SDSS J234841.38−004022.1) were also on our target list and classified as L4 and L1.5, respectively. We conclude that most of their objects are still detectable at individual epochs as we used in our HPM survey.
2. The low-resolution (and relatively low signal-to-noise) spectra of our faint targets observed with FORS1@VLT allowed us to classify them as early-L (13 objects) , late-M (8), mid-M (13) dwarfs, and CWDs (4). In addition, two previously known L dwarfs were reclassified by us. None of the 38 spectra looked like those of the three ultracool (>sdM7) subdwarf spectra observed by us for comparison, but 9 out of 13 mid-M dwarfs were alternatively classified as subdwarfs (sdM7 and earlier types) from a comparison with additional subdwarf templates. Relatively uncertain spectral index measurements also hint at a possible subdwarf nature of seven M dwarfs. One mid-M dwarf is likely a very low-metallicity (usdM) object or may have an unresolved white dwarf companion.
3. The number of L dwarfs in the S82 area, which before our study was already one of the best investigated fields in the sky, has been further increased (from 22 to 35). The newly added L dwarfs are preferentially thick disk and halo objects as are the new late-M dwarfs and CWDs found in S82. The nearest new object is an L4 dwarf (SDSS J011014.30+010619.1) at 64 pc. All other new M and L dwarfs have spectroscopic distance estimates above 100 pc.
4. The re-discovery of all formerly known L dwarfs and even of some T dwarfs in S82, including the L 8 dwarf SDSSp J010752.33+004156.1 and the T 4.5 dwarf SDSS J020742.48+000056.2 with trigonometric parallaxes (Vrba et al. 2004) placing them at 16 and 29 pc, respectively, shows that our HPM survey was sensitive to discovering very nearby objects, too. *However, we failed to detect additional very nearby objects.* For two previously known objects reclassified by us, the L 4.5 dwarf 2MASS J00521232+0012172 and the L 9 dwarf SDSSp J023617.93+004855.0, we have determined new spectroscopic distances of 53 pc (formerly 81 pc) and 18 pc (formerly 21 pc), respectively.
5. On the one hand, we may have been just unlucky in finding new L-type neighbours of the Sun since our survey covered only 1/150 of the sky and the total number of missing L dwarfs in the Solar neighbourhood (within about 50 pc) may be of the order of several hundreds. On the other hand, the S82 area had already been well-investigated for the apparently brighter and consequently more nearby L dwarfs. Using the L and T dwarf compendium by Gelino et al. (2008) and the M_J/spectral type relation given in Dahn et al. (2002), we have estimated that about 400 of the known L dwarfs have spectroscopic distances of less than 50 pc. 11 of them (seven L 0–L 4.5 and four L 5.5–L 9.5 dwarfs) lie in the S82 area, which corresponds to a 4 times higher surface density than the average. Therefore, we conclude that the census of nearby L dwarfs in S82 was probably already near-complete before our study. The space density of L dwarfs determined from the 11 objects within 50 pc falling in the S82 area is about 0.003 pc^{-3}. This is comparable with the value we get from the probably more complete list of about 200 L dwarfs with spectroscopic distances within 25 pc in Gelino et al. (2008), again using the Dahn et al. (2002) M_J/spectral type relation.
6. With our deep HPM survey we have discovered preferentially high-velocity late-M and L dwarfs. However, the optical spectra of these objects do not show indications of a lower metallicity typical of ultracool subdwarfs. As long as we have no infrared data on the new fast late-M and L dwarfs, we cannot say whether they are unusually blue (according to specific near-infrared spectral features) or blue photometric outliers (acording to their $J - K_s$ colours) (cf. Faherty et al. 2008). Our findings suggest that there may exist a population of normal-metallicity ultracool halo objects.
7. 10 of the 38 HPM objects have uncertain proper motions. Most of these uncertain proper motion objects turned out to be mid-M dwarfs at large distances. Most of them have been alternatively classified as subdwarfs or can be considered as subdwarf candidates, which may in fact have large velocities. However, the extremely high tangential velocities (700...2500 km s^{-1}) of nine objects suggest an overestimation of their proper motions. A more careful investigation of the kinematics of these sources makes sense only after a verification of their proper motions with additional epoch measurements. When the high proper motions are confirmed we would also need higher resolution and signal-to-noise spectra to investigate their metallicities and radial velocities.
8. Follow-up observations (better spectroscopy and near-infrared photometry allowing a fit of the observed spectral energy distribution with CWD atmosphere models to determine the effective temperatures) are needed to better characterise the four new CWDs. Trigonometric parallax measurements are challenging in view of their faint magnitudes and possible large distances, but would provide the ultimate values of their absolute magnitudes. Their estimated distances of more than 100 pc are based on the assumption that their

absolute magnitudes compare with other CWDs detected in the SDSS.

9. If we consider the optimistic case that all four new CWDs are Galactic halo members within 170 pc, we can determine a space density of 2.9×10^{-5} pc^{-3} *for halo CWDs alone*, which is almost exactly the same number as the density of 3.0×10^{-5} pc^{-3} derived by Gates et al. (2004) for a mix of *all* CWDs in various Galactic components. Even with the conservative assumtion that only two of our CWDs are representatives of the halo population the estimated space density of halo CWDs already reaches 50% of the above cited value. Nevertheless, our derived space density of halo CWDs is consistent with other estimates indicating that ancient CWDs do not contribute significantly to the baryonic fraction of the dark halo of the Galaxy (see Carollo et al. 2007 and references therein). Our estimate of the density of halo CWDs corresponds to less than 0.4% of the local dark matter density (0.0079 $M_\odot$ pc^{-3}) adopted by Torres et al. (2008).

Acknowledgements. We thank the referee, Dr. Adam Burgasser, for his very helpful detailed comments and suggestions. We thank Doug Finkbeiner for his help accessing the SDSS data at Princeton University, Fernando Comerón and the ESO User Support Department for their help during phase 2 preparation of the service mode observations with the VLT, and the observers at ESO for carrying out these observations. We also thank Daniel Bramich, Evalyn Gates, David Hogg and Donald Schneider for helpful comments. Funding for the SDSS and SDSS-II has been provided by the Alfred P. Sloan Foundation, the Participating Institutions, the National Science Foundation, the U.S. Department of Energy, the National Aeronautics and Space Administration, the Japanese Monbukagakusho, the Max Planck Society, and the Higher Education Funding Council for England. The SDSS Web Site is http://www.sdss.org/. The SDSS is managed by the Astrophysical Research Consortium for the Participating Institutions. The Participating Institutions are the American Museum of Natural History, Astrophysical Institute Potsdam, University of Basel, University of Cambridge, Case Western Reserve University, University of Chicago, Drexel University, Fermilab, the Institute for Advanced Study, the Japan Participation Group, Johns Hopkins University, the Joint Institute for Nuclear Astrophysics, the Kavli Institute for Particle Astrophysics and Cosmology, the Korean Scientist Group, the Chinese Academy of Sciences (LAMOST), Los Alamos National Laboratory, the Max-Planck-Institute for Astronomy (MPIA), the Max-Planck-Institute for Astrophysics (MPA), New Mexico State University, Ohio State University, University of Pittsburgh, University of Portsmouth, Princeton University, the United States Naval Observatory, and the University of Washington. This publication makes use of data products from the Two Micron All Sky Survey, which is a joint project of the University of Massachusetts and the Infrared Processing and Analysis Center/California Institute of Technology, funded by the National Aeronautics and Space Administration and the National Science Foundation.

References

Abazajian, K. N., Adelman-McCarthy, J. K., Agüeros, M. A., et al. 2008 [arXiv:0812.0649]
Adelman-McCarthy, J. K., Agüeros, M. A., Allam, S. S., et al. 2008, ApJS, 175, 297
Appenzeller, I., Fricke, K., Fürtig, W., et al. 1998, Messenger, 94, 1
Artigau, É., Doyon, R., Lafrenière, D., et al. 2006, ApJ, 651, L57
Berriman, B., Kirkpatrick, D., Hanisch, R., Szalay, A., & Williams, R. 2003, IAUJD, 8, 60
Bramich, D. M., Vidrih, S., Wyrzykowski, L., et al. 2008, MNRAS, 386, 887
Burgasser, A. J., & Kirkpatrick, J. D. 2006, ApJ, 645, 1485
Burgasser, A. J., Kirkpatrick, J. D., Brown, M. E., et al. 2002, ApJ, 564, 421
Burgasser, A. J., Kirkpatrick, J. D., Burrows, A., et al. 2003, ApJ, 592, 1186
Burgasser, A. J., Geballe, T. R., Leggett, S. K., Kirkpatrick, J. D., & Golimowski, D. A. 2006, ApJ, 637, 1067
Burgasser, A. J., Cruz, K. L., & Kirkpatrick, J. D. 2007, ApJ, 657, 494
Carollo, D., Bucciarelli, B., Hodgkin, S. T., et al. 2006, A&A, 448, 579
Carollo, D., Bucciarelli, B., & Hodgkin, S. T., 2007, 15th European Workshop on White Dwarfs, ASP Conf. Ser., 372, 113
Chiu, K., Liu, M. C., Jiang, L., et al. 2008, MNRAS, 385, L53
Cushing, M. C., & Vacca, W. D. 2006, AJ, 131, 1797
Cruz, K. L., & Reid, I. N. 2002, AJ, 123, 2828
Cruz, K. L., Reid, I. N., Liebert, J., et al. 2003, AJ, 126, 2421
Dahn, C. C., Harris, H. C., Vrba, F. J., et al. 2002, AJ, 124, 1170
Dahn, C. C., Harris, H. C., Levine, S. E., et al. 2008, ApJ, 686, 548
Delfosse, X., Tinney, C. G., Forveille, T., et al. 1997, A&A, 327, L25
Delorme, P., Delfosse, X., Albert, L., et al. 2008, A&A, 482, 961
Epchtein, N., de Batz, B., Capoani, L., et al. 1997, The Messenger, 87, 27
Faherty, J. K., Burgasser, A. J., Cruz, K. L., et al. 2009, AJ, 137, 1
Fan, X., Knapp, G. R., Strauss, M. A., et al. 2000, AJ, 119, 928
Finkbeiner, D. P., Padmanabhan, N., Schlegel, D. J., et al. 2004, AJ, 128, 2577
Flynn, C., Holopainen, J., & Holmberg, J. 2003, MNRAS, 339, 817
Folkes, S. L., Pinfield, D. J., Kendall, T. R., & Jones, H. R. A. 2007, MNRAS, 378, 901
Frieman, J. A., Bassett, B., Becker, A., et al. 2008, AJ, 135, 338
Fukugita, M., Ichikawa, T., Gunn, J. E., et al. 1996, AJ, 111, 1748
Gates, E., Gyuk, G., Harris, H. C., et al. 2004, ApJ, 612, L129
Geballe, T. R., Knapp, G. R., Leggett, S. K., et al. 2002, ApJ, 564, 466
Gelino, C. R., Kirkpatrick, J. D., & Burgasser, A. J. 2008, online database for 649 L and T dwarfs at DwarfArchives.org (status: 22 April, 2008)
Gizis, J. E. 1997, AJ, 113, 806
Gizis, J. E., & Harvin, J. 2006, AJ, 132, 2372
Gizis, J. E., Reid, I. N., & Hawley, S. L. 2002, AJ, 123, 3356
Gunn, J. E., Carr, M., Rockosi, C., et al. 1998, AJ, 116, 3040
Gunn, J. E., Siegmund, W. A., Mannery, E. J., et al. 2006, AJ, 131, 2332
Hall, P. B., Kowalski, P. M., Harris, H. C., et al. 2008, AJ, 136, 76
Hambly, N. C., Smartt, S. J., & Hodgkin, S. T. 1997, ApJ, 489, L157
Hambly, N. C., MacGillivray, H. T., Read M. A., et al. 2001a, MNRAS, 326, 1279
Hambly, N. C., Irwin, M. J., & MacGillivray, H. T. 2001b, MNRAS, 326, 1295
Hambly, N. C., Davenhall, A. C., Irwin, M. J., & MacGillivray, H. T. 2001c, MNRAS, 326, 1315
Hambly, N. C., Henry, T. J., Subasavage, J. P., Brown, M. A., & Jao, W.-C. 2004, AJ, 128, 437
Hamuy, M., Suntzeff, N. B., Heathcote, S. R., et al. 1994, PASP, 106, 566
Harris, H. C., Dahn, C. C., Vrba, F. J., et al. 1999, ApJ, 524, 1000
Harris, H. C., Hansen, B. M. S., Liebert, J., et al. 2001, ApJ, 549, L109
Harris, H. C., Gates, E., Gyuk, G., et al. 2008, ApJ, 679, 697
Hawley, S. L., Covey, K. R., Knapp, G. R., et al. 2002, AJ, 123, 3409
Henry, T. J., Walkowicz, L. M., Barto, T. C., & Golimowski, D. A. 2002, AJ, 123, 2002
Henry, T. J., Jao, W.-C., Subasavage, et al. 2006, AJ, 132, 2360
Hertzsprung, E. 1905, Zeit. Phot., 3, 429
Hogg, D. W., Finkbeiner, D. P., Schlegel, D. J., & Gunn, J. E. 2001, AJ, 122, 2129
Ibata, R., Irwin, M., Bienaymé, O., Scholz, R., & Guibert, J. 2000, ApJ, 532, L41
Ivezić, Ž., Lupton, R. H., Schlegel, D., et al. 2004, AN, 325, 583
Kendall, T. R., Jones, H. R. A., Pinfield, D. J., et al. 2007, MNRAS, 374, 445
Kilic, M., Munn, J. A., Harris, H. C., et al. 2006, AJ, 131, 582
Kirkpatrick, J. D. 2005, ARA&A, 43, 195
Kirkpatrick, J. D., Reid, I. N., Liebert, J., et al. 1999, ApJ, 519, 802
Knapp, G. R., Leggett, S. K., Fan, X., et al. 2004, AJ, 127, 3553
Lang, D., Hogg, D. W., Jester, S., Rix, H.-W. 2008 [arXiv:0808.4004]
Lawrence, A., Warren, S. J., Almaini, O., et al. 2007, MNRAS, 379, 1599
Leggett, S. K., Ruiz, M. T., Bergeron, P. 1998, ApJ, 497, 294
Lépine, S., & Shara, M. M. 2005, AJ, 129, 1483
Lépine, S., & Scholz, R.-D. 2008, ApJ, 681, L33
Lépine, S., Rich, R. M., & Shara, M. M. 2003, ApJ, 591, L49
Lépine, S., Shara, M. M., & Rich, R. M. 2004, ApJ, 602, L125
Lépine, S., Rich, R. M., & Shara, M. M. 2005, ApJ, 633, L121
Lépine, S., Rich, R. M., & Shara, M. M. 2007, ApJ, 669, 1235
Liu, M. C., Wainscoat, R., Martín, E. L., Barris, B., & Tonry, J. 2002, ApJ, 568, L107
Lodieu, N., Pinfield, D. J., Leggett, S. K., et al. 2007, MNRAS, 379, 1423
Looper, D. L., Kirkpatrick, J. D., & Burgasser, A. J. 2007, AJ, 134, 1162
Lupton, R. H., Gunn, J. E., & Szalay, A. S. 1999, AJ, 118, 1406
Lupton, R., Gunn, J. E., Ivezić, Z., Knapp, G. R., & Kent, S. 2001, in Astronomical Data Analysis Software and Systems X, ed. F. R. Harnden Jr., F. A. Primini, & H. E. Payne (San Francisco: ASP), ASP Conf. Ser., 238, 269
Luyten, W. J. 1922, Lick Obs. Bull., 10, 135
Luyten, W. J. 1979a, LHS Catalogue: a catalogue of stars with proper motions exceeding 0.5″ annually, University of Minnesota, Minneapolis
Luyten W. J. 1979b, New Luyten Catalogue of Stars with Proper Motions Larger than Two Tenths of an Arcsecond, Univ. Minnesota, Minneapolis
Luyten W. J., & Hughes H. S. 1980, NLTT first supplement, Univ. Minnesota, Minneapolis
Martín, E. L., Delfosse, X., Basri, G., et al. 1999, AJ, 118, 2466
Martín, E. L., Brandner, W., Bouy, H., et al. 2006, A&A, 456, 253
Méndez, R. A. 2002, A&A, 395, 779
Metchev, S. A., Kirkpatrick, J. D., Berriman, G. B., & Looper, D. 2008, ApJ, 676, 1281

Monet, D. G., Dahn, C. C., Vrba, F. J., et al. 1992, AJ, 103, 638
Monet, D. G., Fisher, M. D., Liebert, J., et al. 2000, AJ, 120, 1541
Monet, D. G., Levine, S. E., Canzian, B., et al. 2003, AJ, 125, 984
Munn, J. A., Monet, D. G., Levine, S. E., et al. 2004, AJ, 127, 3034
Oppenheimer, B. R., Hambly, N. C., Digby, A. P., et al. 2001, Science, 292, 698
Padmanabhan, N., Schlegel, D. J., Finkbeiner, D. P., et al. 2008, ApJ, 674, 1217
Phan-Bao, N., Bessell, M. S., Martín, E. L., et al. 2008, MNRAS, 383, 831
Pier, J. R., Munn, J. A., Hindsley, R. B., et al. 2003, AJ, 125, 1559
Pokorny, R. S., Jones, H. R. A., & Hambly, N. C. 2003, A&A, 397, 575
Pokorny, R. S., Jones, H. R. A., Hambly, N. C., & Pinfield, D. J. 2004, A&A, 421, 763
Raymond, S. N., Szkody, P., Hawley, S. L., et al. 2003, AJ, 125, 2621
Reid, I. N. 2005, ARA&A, 43, 247
Reid, I. N., Hawley, S. L., & Gizis, J. E. 1995, AJ, 110, 1838
Reid, I. N., Sahu, K. C., & Hawley, S. L. 2001, ApJ, 559, 942
Reid, I. N., Gizis, J. E., & Hawley, S. L. 2002, AJ, 124, 2721
Rowell, N. R., Kilic, M., & Hambly, N. C. 2008, MNRAS, 385, L23
Ruiz, M. T., Leggett, S. K., & Allard, F. 1997, ApJ, 491, L107
Salim, S., Rich, R. M., Hansen, B. M., et al. 2004, ApJ, 601, 1075
Schmidt, S. J., Cruz, K. L., Bongiorno, B. J., Liebert, J., & Reid, I. N. 2007, AJ, 133, 2258
Schneider, D. P., Knapp, G. R., Hawley, S. L., et al. 2002, AJ, 123, 458
Scholz, R.-D., Irwin, M., Ibata, R., et al. 2000, A&A, 353, 958
Scholz, R.-D., Szokoly, G. P., Andersen, M., Ibata, R., & Irwin, M. J. 2002, ApJ, 565, 539
Scholz, R.-D., McCaughrean, M. J., Lodieu, N., & Kuhlbrodt, B. 2003, A&A, 398, L29
Scholz, R.-D., Lehmann, I., Matute, I., & Zinnecker, H. 2004a, A&A, 425, 519
Scholz, R.-D., McCaughrean, M. J., & Lodieu, N. 2004b, A&A, 428, L25
Scholz, R.-D., Meusinger, H., Jahreiß, H. 2005, A&A, 442, 211
Sivarani, T., Kembhavi, A. K., & Gupchup, J. 2004, ApJ Lett., submitted (this manuscript was previously available at: http://www.iucaa.ernet.in/~gupchup/final_ApjL.pdf)
Skrutskie, M. F., Cutri, R. M., Stiening, R., et al. 2006, AJ, 131, 1163
Smith, J. A., Tucker, D. L., Kent, S., et al. 2002, AJ, 123, 2121
Smith, M. C., Ruchti, G. R., Helmi, A., et al. 2007, MNRAS, 379, 755
Stoughton, Ch., Lupton, R. H., Bernardi, M., et al. 2002, AJ, 123, 485
Subasavage, J. P., Henry, T. J., Hambly, N. C., Brown, M. A., & Jao, W.-Ch. 2004, AJ, 130, 1658
Subasavage, J. P., Henry, T. J., Bergeron, P., Dufour, P., & Hambly, N. C. 2008, AJ, 136, 899
Tinney, C. G. 1998, MNRAS, 296, L42
Torres, S., Camacho, J., Isern, J., & García-Berro, E. 2008, A&A, 486, 427
Tucker, D. L., Kent, S., Richmond, M. W., et al. 2006, AN, 327, 821
van Altena, W. F., Lee, J. T., & Hoffleit, E. D. 1995, The General Catalogue of Trigonometric Stellar Parallaxes, Fourth Edition, Yale University Observatory, available at http://vizier.u-strasbg.fr/viz-bin/Cat?I/238A
Vrba, F. J., Henden, A. A., Luginbuhl, C. B., et al. 2004, AJ, 127, 2948
Vidrih, S., Bramich, D. M., Hewett, P. C., et al. 2007, MNRAS, 382, 515
Warren, S. J., Mortlock, D. J., Leggett, S. K., et al. 2007, MNRAS, 381, 1400
West, A. A., Walkowicz, L. M., & Hawley, S. L. 2005, PASP, 117, 706
West, A. A., Hawley, S. L., Bochanski, J. J., et al. 2008, 135, 785
York, D. G., Adelman, J., Anderson, J. E., et al. 2000, AJ, 120, 1579